ydroxylase Domain-2 Gene. Mol Ther. 16(7):1227-34 (2008)
Miyata K, Oba M, Kano MR, Fukushima S, Vachutinsky Y, Han M, Koyama H, Miyazono K, Nishiyama N, Kataoka K. Polyplex Micelles from Triblock Copolymers Composed of Tandemly Aligned Segments with Biocompatible, Endosomal Escaping, and DNA-Condensing Functions for Systemic Gene Delivery to Pancreatic Tumor Tissue. Pharm Res. 25(12):2924-36 (2008)
Kano MR, Komuta Y, Iwata C, Oka M, Shirai Y, Morishita Y, Ouchi Y, Kataoka K, Miyazono K. Comparison of the effects of the kinase inhibitors, Imatinib, Sorafenib, and TGF-β receptor inhibitor, on extravasation of nanoparticles from neovasculature. Cancer Sci. 100(1):173-80 (2009)
A. Komuro, M. Yashiro, C. Iwata, Y. Morishita, E. Johansson, Y. Matsumoto, A. Watanabe, H. Aburatani, H. Miyoshi, K. Kiyono, Y. - Shirai, H. I. Suzuki, K. Hirakawa, M. R. Kano, K. Miyazono, Diffuse-type gastric carcinoma: progression, angiogenesis, and transforming growth factor beta signaling. J. Natl. Cancer Inst. (2009) 101 (8) 592-604
M. Han, M. Oba, N. Nishiyama, M. R. Kano, S. Kizaka-Kondoh, K. Kataoka, Enhanced percolation and gene expression in tumor hypoxia by PEGylated polyplex micelles. Mol. Ther. (2009) 17 (8) 1404-1410
M. Kumagai, M. R. Kano, Y. Morishita, M. Ota, Y. Imai, N. Nishiyama, M. Sekino, S. Ueno, K. Miyazono, K. Kataoka, Enhanced magnetic resonance imaging of experimental pancreatic tumor in vivo by block copolymer-coated magnetite nanoparticles with TGF-beta inhibitor. J. Control Release. (2009) 140 (3) 306-311
K. Kiyono, H. I. Suzuki, Y. Morishita, A. Komuro, C. Iwata, M. Yashiro, K. Hirakawa, M. R. Kano, K. Miyazono, c-Ski overexpression promotes tumor growth and angiogenesis through inhibition of transforming growth factor-beta signaling in diffuse-type gastric carcinoma. Cancer Sci. (2009) 100 (10) 1809-1816
K. Kiyono, H. I. Suzuki, H. Matsuyama, Y. Morishita, A. Komuro, M. R. Kano, K. Sugimoto, K. Miyazono, Autophagy is activated by TGF-beta and potentiates TGF-beta-mediated growth inhibition in human hepatocellular carcinoma cells. Cancer Res. (2009) 69 (23) 8844-8852
Y. Vachutinsky, M. Oba, K. Miyata, S. Hiki, M. R. Kano, N. Nishiyama, H. Koyama, K. Miyazono, K. Kataoka, Antiangiogenic gene therapy of experimental pancreatic tumor by sFlt-1 plasmid DNA carried by RGD-modified crosslinked polyplex micelles. J. Control Release. (2010) in press
M. Oba, Y. Vachutinsky, K. Miyata, M. R. Kano, S. Ikeda, N. Nishiyama, K. Itaka, K. Miyazono, H. Koyama, K. Kataoka, Antiangiogenic gene therapy of solid tumor by systemic injection of polyplex micelles loading plasmid DNA encoding soluble flt-1. Mol. Pharm. (2010) 7 (2) 501-509
狩野光伸・宮園浩平　血管におけるTGF-βファミリーシグナル　医学のあゆみ2008:223(12); 1037-1042
狩野光伸　腫瘍発育、血管新生、治療反応性への動脈硬化と血管老化の影響　分子細胞治療2008:7(1)79-80
狩野光伸・宮園浩平　EMT制御と分子標的薬　実験医学2009:27(5)653-660
狩野光伸　腫瘍血管正常化と血管壁細胞　血管医学　2009:10(4)349-355

2.　学会発表
第98回日本病理学会総会、「難治腫瘍モデルを用いた治療法の開拓」京都、2009年5月1日

第25回日本DDS学会、Histological characteristics of tumor and effect of nanoDDS.　東京、2009年7月3日

2009年度がん若手ワークショップ、Treating “untreatable” tumors、蓼科、2009年9月5日

第68回日本癌学会学術総会、「腫瘍脈管の機能解析を目指した動物モデル」横浜、2009年10月2日

第17回血管生物医学会、ナノテクノロジーで腫瘍血管構築をとらえなおす、東京、2009年10月8日

放射線医学総合研究所シンポジウム「生体イメージングの未来」、「難治腫瘍とナノDDS」、千葉、2009年11月27日

星薬科大学オープンリサーチシンポジウム、「難治固形腫瘍にナノDDS製剤を到達させるには：腫瘍血管の研究を通じて」、東京、2009年12月5日

第1回バイオクリエーション研究会特別シンポジウム、「Bio-creationによる難病解明」、愛媛、2010年1月25日

第99回日本病理学会総会、がん難治性の原因をナノテクノロジーと病理学によって捉えなおす、2010年4月29日

H. 知的財産権の出願・登録状況
1. 特許取得
片岡一則, 熊谷 康顕, 狩野 光伸, 関野 正樹, 松浦 哲也, 宮園 浩平, 西山 伸宏、腫瘍撮像用MRI造影剤、特開2008-28027

別紙4-4

厚生労働科学研究費補助金（ナノメディシン研究事業）
分担研究報告書

血管内腔からがん組織への高効率・特異的移行を実現する革新的DDSの創成と脳腫瘍標的治療への展開
（ヒト脳腫瘍組織の分子病理学的検討）

研究分担者　西原　広史　北海道大学大学院医学系研究科　特任准教授

研究要旨
本研究は、脳腫瘍血管構築の特異性を明らかにしながら、血管内皮細胞のトランスサイトーシスによるミセル型DDSの高い集積性を利用し、より効果的な脳腫瘍治療薬開発を目指すものであるが、これらの研究モデル開発及び開発薬剤の投与にあたり、実際のヒト脳腫瘍組織での組織構築を解析し、比較検討を行うことが、その有効性検証に不可欠である。本年度はDDSのターゲットとなる脳腫瘍特異的な血管構築の解析を行った。

A．研究目的

脳腫瘍はBlood Tumor Barriorの存在により、従来の抗癌剤治療薬の効果が低い癌である。本研究は、脳腫瘍血管の構築を明らかにしながら、ナノバイオテクノロジーを用いて新しいDrug Delivary Systemを構築し、より効果的な脳腫瘍治療薬開発を目指すものである。

B．研究方法

実際のヒト脳腫瘍標本における血管構築を免疫染色及び電子顕微鏡により検討することで、まずDDSの観点から見た脳腫瘍の特徴を把握することを計画した。

具体的には、比較的抗癌剤への感受性があり予後良好とされているOligodendrogliomaと、抗癌剤感受性が低く予後も不良である、Astrocytic tumorの血管パターンの比較を行った。用いた検体は、当教室にて過去に診断がなされた脳腫瘍切除病理標本２０例を用い、免疫染色（血管内皮マーカー；CD31、CD34、壁細胞マーカー；αSMA、Desmin、PDGFRβ、TGFβシグナルの検出；phospho-Smad2）、及び透過型電子顕微鏡による観察を行った。

（倫理面への配慮）
本研究で用いられるヒト病理検体はすべて研究開始前に人体から採取された試料であり、患者個人に不利益・危険性が及ぶことはない。しかし、人権擁護の観点から原則として研究開始前までに当該患者から試料の利用に係る同意を受けるものとし、同意を受けることが出来ない場合には臨床研究に関する倫理指針に基づき、本学倫理委員会の承認の下に研究を遂行する。同時に、これらの研究活動を当教室のホームページに公表し、もし患者から自身の検体の使用停止の申し入れがあった場合には速やかにその検体の使用を中止することとしている。また、成果発表等の際には個人を特定できないよう最大限の配慮をした。

C．研究結果

１）ヒト脳腫瘍病理検体の免疫染色
Astrocytic tumorの代表であるGlioblastoma（GBM)では、従来血管内皮の増生からなるとされているglomeruloid vesselという肥厚血管を認める。一方、oligodendroglial tumorでは、Chicken wire vascular networkと呼ばれる細い血管網の発達が特徴である。まずこれらの血管構造を免疫組織化学的に検討し、構成細胞の同定を行った。

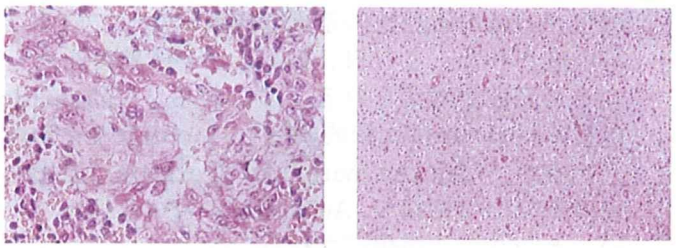

図１　左がGloemruloid血管、　右がChecken wire血管

その結果、Glomeruloid vesselを構成する細胞の大部分は、αSMA陽性、PGDFRβ陽性の、いわゆるPericyteが大部分で、CD34陽性の血管内皮細胞は血管内腔を1層覆うのみで、増生は顕著ではなかった。（図２参照）

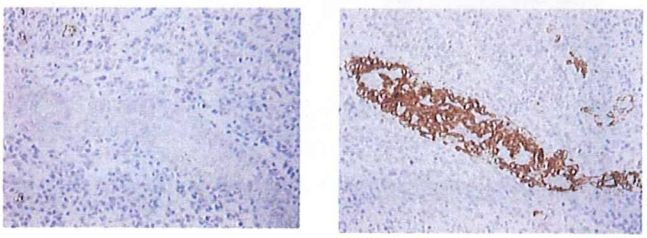

図２　左は血管内皮（CD34）、右はPericyte(Actin)
大部分はActin陽性のPericyteで構成されている。

一方、Chicken wire vascular networkを構成する細血管については、一層の血管内皮（CD34陽性）の外層に、一層のPDGFRβ陽性の薄いPericyteが見られるが、この細胞にはαActinは陰性であった（図3）。

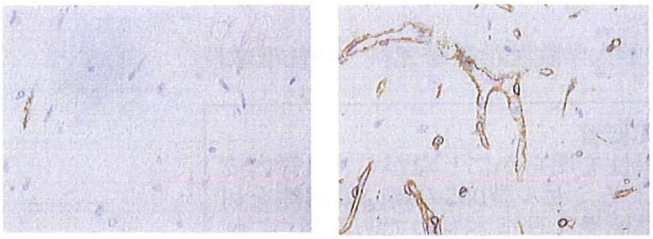

図３　Chicken wire 血管の染色。左はαSMA、右はPDGFRβ。

以上の結果から、両者の血管壁には、Pericyteの量の違いと同時に、αActinの染色性という質的な違いが認められることが判明した。これは今までには報告されていない事項である。

２）電子顕微鏡による脳腫瘍特異的血管の観察

上記で認められたPericyteの質的差異の原因を探求するために、電子顕微鏡による観察を行った。用いた資料は、ホルマリン固定病理検体をグルタールアルデヒドで再固定したものである。その結果、Glomeruloid血管に見られる肥厚したPericyteには、不規則なFilamentが多数認めらたのに対して（図４）、Chicken wire血管のPericyteではそのようなFilamentは全く認められなかった（図５）。このFilamentがαActinの染色性の差異の原因になっていることが示唆された。これは、Pericyteの成熟度を表している可能性が考えられる。すなわち、Glomeruloid血管のPericyteは比較的成熟し、Actin線維を形成しているが、Chicken wire血管のPericyteは未熟あるいは未分化な細胞で、Actin線維の合成を行っていない、ということが想定される。

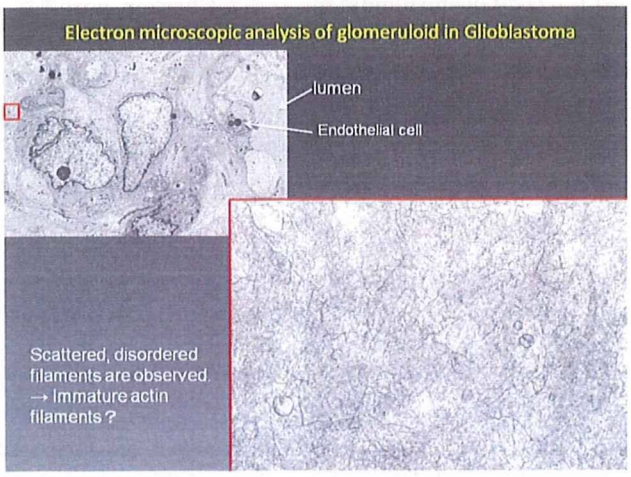

図４　Glomeruloid血管の電子顕微鏡像

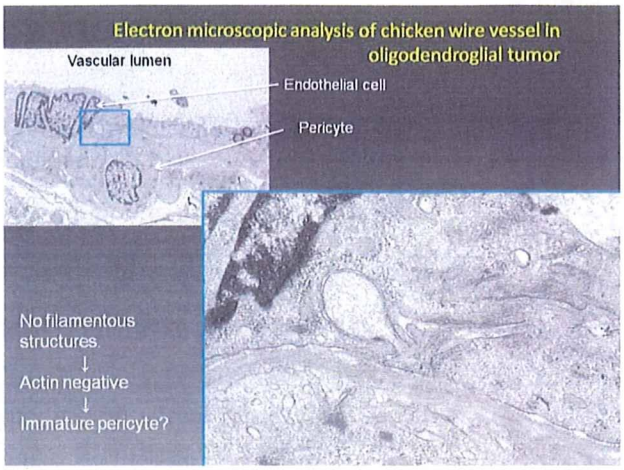

図５　Chicken wire血管の電子顕微鏡像

D．考察

悪性膠芽腫のうち、Astrocytic tumorは予後不良で、Oligodendroglial tumorは比較的予後良好と言われているが、その理由は腫瘍細胞自体の特性によるのか、あるいはその背景組織にあるのかについては全く定説がない。しかし、本研究の結果から、少なくとも両者間の背景には大きな血管構造の差異が認められ、もしこの周皮細胞の量や特性が抗癌剤の浸透性に影響していると仮定すると、その予後の違いは抗癌剤のDrug deliveryの違いによって生じている可能性が考えられる。これを証明するには今後、Pecicyteを用いたIn vitro実験モデルでの薬剤透過性実験を行うと同時に、血管周皮細胞を伴った血管新生を示す動物実験モデルを開拓し、この血管周皮細胞による抗癌剤の浸透性の検討を行う必要がある。さらに、現在、これらの血管パターンに応じて、実際の脳腫瘍組織を分類し、その治療成績・予後との相関を開始した。その結果、もし血管パターンと予後に相関が認められるようであれば、これは我々の仮説を証明することになり、この脳腫瘍特異的血管と治療抵抗性のメカニズムを解明することの重要性を確証することになる。

E．結論

今年度の研究により、ヒト脳腫瘍に特徴的な血管構築のうち、その悪性度と相関するのは肥厚した血管壁のPericyteにあることが示唆された。さらに、これらの周皮細胞にはTGFβシグナルが認められるため、TGFβ阻害剤の有効性に関与していることが示唆された。

G．研究発表

1. 論文発表

1．Nishihara H, Nakasato M, Sawa H, Mura kami H, Yamamoto D, Moriyama K, Kato N, Hashimoto I, Kamada H, Tanaka S. A case of central nervous system lympho matoid granulomatosis; characteristics of PET imaging and pathological findings. J Neurooncol. 2009 Jun;93(2):275-8.

2．Kimura T, Sakai M, Tabu K, Wang L, Ts unematsu R, Tsuda M, Sawa H, Nagashi ma K, Nishihara H, Hatakeyama S, Naka yama K, Ladanyi M, Tanaka S, Nakayam a KI. Human synovial sarcoma proto-onco gene Syt is essential for early embryonic development through the regulation of cell migration. Lab Invest. 2009 Jun;89(6):645 -56.

3．Watanabe T, Tsuda M, Makino Y, Konsta ntinou T, Nishihara H, Majima T, Minam i A, Feller SM, Tanaka S. Crk adaptor pr otein-induced phosphorylation of Gab1 on tyrosine 307 via Src is important for orga nization of focal adhesions and enhanced cell migration. Cell Res. 2009 May;19(5): 638-50.

4．Takiyama A, Wang L, Tanino M, Kimura T, Kawagishi N, Kunieda Y, Katano H, Nakajima N, Hasegawa H, Takagi T, Nis hihara H, Sata T, Tanaka S. Sudden de ath of a patient with pandemic influenza (A/H1N1pdm) virus infection by acute res piratory distress syndrome. Jpn J Infect Dis. 2010 Jan;63(1):72-4.

5．Tabu K, Kimura T, Sasai K, Wang L, Biz en N, Nishihara H, Taga T, Tanaka S. Analysis of an alternative human CD133 promoter reveals the implication of Ras/E RK pathway in tumor stem-like hallmarks. Mol Cancer. 2010 Feb 19;9(1):39.

6．Wang L, Nishihara H, Kimura T, Kato Y, Tanino M, Nishio M, Obara M, Endo T, Koike T, Tanaka S. DOCK2 regulates cel l proliferation through Rac and ERK activ ation in B cell lymphoma. Biochem Biop hys Res Commun. 2010 Mar 27. [Epub ah ead of print]

2. 学会発表

1．5月8－9日　(福岡)　第27回　日本脳腫瘍病理学会総会；　西原　広史、狩野　光伸、田中、伸哉；　脳腫瘍血管壁の組織病理学的解析：Glomeru loid vesselは肥厚した幼若なPericyteで構成されている

2．7月３日　(東京)　第25回日本DDS学会学術集会　ワークショップDDSとがん組織（間質、脈管）　西原　広史　Pathological analysis for cancer-mesenchymal and vascular structure associated with drug delivery system.　(招待講演)

3．10月1－3日　(横浜)　第68回　日本癌学会学術総会；　Hiroshi Nishihara, Kazuo Nagashima, Shinya Tanaka
CNS-lymphomatoid granulomatosis; as a primary lesion for CNS-T cell lymphoma

4．12月13-15日　(アメリカ、サンディエゴ)　AACR Special Conference on Genetics and Biology of Brain Cancers；　Hiroshi Nishihara, Mitsunobu R. Kano, Hiromi Kanno, Shinya Tanaka
Clinicopathological analysis for glioma-specific vascular structures.

H．知的財産権の出願・登録状況

1. 特許取得

なし

別紙５

研究成果の刊行に関する一覧表

雑誌

発表者氏名	論文タイトル名	発表誌名	巻号	ページ	出版年
M. Oba, M. R. Kano N. Nishiyama K. Kataoka, et al.	Antiangiogenic gene therapy of solid tumor by systemic injection of polyplex micelles loading plasmid DNA encoding soluble Flt-1.	Mol. Pharm.	7	501-509	2010
S. Hiki, K. Kataoka, et al.	Versatile and selective synthesis of "Click Chemistry" compatible heterobifunctional poly(ethylene glycol)s possessing azide and alkyne functionalities.	Bioconjugate. Chem.	21	248-254	2010
M. Kumagai, M. R. Kano N. Nishiyama K. Kataoka, et al.	Enhanced magnetic resonance imaging of experimental pancreatic tumor in vivo by block-copolymer-coated magnetite nanoparticles with TGF-beta inhibitor.	J. Control. Release	140	306-311	2009
M. Han, N. Nishiyama M. R. Kano K. Kataoka, et al.	Enhanced percolation and gene expression in tumor hypoxia by PEGylated polyplex micelles.	Mol. Ther.	17	1404-1410	2009
H. Ikushima, Y. Ino, et al.	TGF-β signaling maintains tumorigenicity of glioma-initiating cells through Sry-related HMG-box factors.	Cell Stem Cell	5	504-514	2009
M.R. Kano, K. Kataoka, et al.	Comparison of the effects of the kinase inhibitors, Imatinib, Sorafenib, and TGF-β receptor inhibitor, on extravasation of nanoparticles from neovasculature.	Cancer Sci.	100	173-180	2009
A. Komuro M.R. Kano, et al.	Diffuse-type gastric carcinoma: progression, angiogenesis, and transforming growth factor beta signaling.	J. Natl. Cancer Inst.	101	592-604	2009

発表者氏名	論文タイトル名	発表誌名	巻号	ページ	出版年
K. Kiyono, M.R. Kano, et al.	Autophagy is activated by TGF-beta and potentiates TGF-beta-mediated growth inhibition in human hepatocellular carcinoma cells.	Cancer Res.	69	8844-8852	2009
T. Kimura, H. Nishihara, et al.	Human synovial sarcoma proto-oncogene Syt is essential for early embryonic development through the regulation of cell migration.	Lab Invest.	89	645-656	2009

molecular pharmaceutics

articles

Antiangiogenic Gene Therapy of Solid Tumor by Systemic Injection of Polyplex Micelles Loading Plasmid DNA Encoding Soluble Flt-1

Makoto Oba,[†] Yelena Vachutinsky,[‡] Kanjiro Miyata,[§] Mitsunobu R. Kano,[||,⊥] Sorato Ikeda,[#] Nobuhiro Nishiyama,[*,§] Keiji Itaka,[§] Kohei Miyazono,[||,⊥] Hiroyuki Koyama,[†] and Kazunori Kataoka[*,†,‡,§,||,#]

Department of Clinical Vascular Regeneration, Graduate School of Medicine, The University of Tokyo, 7-3-1 Hongo, Bunkyo, Tokyo 113-8655, Japan, Department of Bioengineering, Graduate School of Engineering, The University of Tokyo, 7-3-1 Hongo, Bunkyo, Tokyo 113-8656, Japan, Center for Disease Biology and Integrative Medicine, Graduate School of Medicine, The University of Tokyo, 7-3-1 Hongo, Bunkyo, Tokyo 113-0033, Japan, Center for NanoBio Integration, The University of Tokyo, 7-3-1 Hongo, Bunkyo, Tokyo 113-8656, Japan, Department of Molecular Pathology, Graduate School of Medicine, The University of Tokyo, 7-3-1 Hongo, Bunkyo-ku, Tokyo 113-8655, Japan, and Department of Materials Engineering, Graduate School of Engineering, The University of Tokyo, 7-3-1 Hongo, Bunkyo, Tokyo 113-8656, Japan

Received September 14, 2009; Revised Manuscript Received January 8, 2010; Accepted February 23, 2010

Abstract: In this study, a polyplex micelle was developed as a potential formulation for antiangiogenic gene therapy of subcutaneous pancreatic tumor model. Poly(ethylene glycol)-poly(L-lysine) block copolymers (PEG-PLys) with thiol groups in the side chain of the PLys segment were synthesized and applied for preparation of disulfide cross-linked polyplex micelles through ion complexation with plasmid DNA (pDNA) encoding the soluble form of vascular endothelial growth factor (VEGF) receptor-1 (sFlt-1), which is a potent antiangiogenic molecule. Antitumor activity and gene expression of polyplex micelles with various cross-linking rates were evaluated in mice bearing subcutaneously xenografted BxPC3 cell line, derived from human pancreatic adenocarcinoma, and polyplex micelles with optimal cross-linking rate achieved effective suppression of tumor growth. Significant gene expression of this micelle was detected selectively in tumor tissue, and its antiangiogenic effect was confirmed by decreased vascular density inside the tumor. Therefore, the disulfide cross-linked polyplex micelle loading sFlt-1 pDNA has a great potential for antiangiogenic therapy against subcutaneous pancreatic tumor model by systemic application.

Keywords: Polymeric micelle; block copolymer; antiangiogenic tumor gene therapy; sFlt-1

Introduction

Antiangiogenic tumor gene therapy is an intensively studied approach to inhibit tumor growth by destructing its neo-vasculature formation.[1,2] Vascular endothelial growth factor (VEGF) is a major proangiogenic molecule, which stimulates angiogenesis via promoting endothelial prolifera-

* To whom correspondence should be addressed. K.K.: tel, +81-3-5841-7138; fax, +81-3-5841-7139; e-mail, kataoka@bmw.t.u-tokyo.ac.jp; The University of Tokyo, Department of Materials Engineering, 7-3-1 Hongo, Bunkyo-ku, Tokyo 113-8656, Japan. N.N.: tel, +81-3-5841-1430; fax, +81-5841-7139; e-mail, nishiyama@bmw.t.u-tokyo.ac.jp.

† Department of Clinical Vascular Regeneration, Graduate School of Medicine.

‡ Department of Bioengineering, Graduate School of Engineering.

§ Center for Disease Biology and Integrative Medicine, Graduate School of Medicine.

|| Center for NanoBio Integration.

⊥ Department of Molecular Pathology, Graduate School of Medicine.

Department of Materials Engineering, Graduate School of Engineering.

10.1021/mp9002317
Published on Web 02/23/2010

tion, survival, and migration. The soluble form of VEGF receptor-1 (fms-like tyrosine kinase-1: Flt-1) is a potent endogeneous molecule, which can be used for antiangiogenic therapy.[3,4] The sFlt-1 binds to VEGF with the same affinity and equivalent specificity as that of the original receptor,[5] however it inhibits its signal transduction.

Gene therapy is becoming a promising strategy to supply consecutive expression of antiangiogenic proteins over a period of time. Indeed, a number of studies have already demonstrated the potential of therapeutic genes encoding angiogenic inhibitors to suppress tumor growth.[6,7] The major challenge in systemic gene therapy, however, is a need for a safe and effective vector system that can deliver the gene to the target tissue and cells with no detrimental side effects. In terms of safety, nonviral gene vectors are gaining popularity over viral vectors, however, their intracellular delivery and transfection potential require further optimization. Recently, several reports were published on *in vivo* nonviral gene therapy utilizing sFlt-1 for inhibition of tumor angiogenesis.[8,9]

Based on these criteria, cross-linked polyplex micelles were designed and prepared through electrostatic interaction of thiolated poly(ethylene glycol)-poly(L-lysine) (PEG-PLys) block copolymers and plasmid DNA (pDNA) encoding sFlt-1. We have previously reported that disulfide cross-links introduced into the polyplex micelle core contribute to the stabilization of its structure in the extracellular entity while facilitating smooth release of the entrapped pDNA, in response to the reductive environment, inside the cells.[10,11] The outer hydrophilic shell layer, formed by PEG segment, increases complex stability in serum, avoiding nonspecific interactions with plasma proteins and reduces polymer toxicity.[12]

In this study, cross-linked polyplex micelles were systemically administered to mice bearing subcutaneously xenografted BxPC3 human pancreatic adenocarcinoma and evaluated for their transfection efficiency. Note that BxPC3 xenografts, as some intractable solid tumors, are characterized by stroma-rich histology,[13] which limits access of therapeutic agents to tumor cells. Thus, the accessibility of endothelial cells by bloodstream makes an antiangiogenic approach an attractive strategy against this model. Here we report a potent tumor growth inhibitory effect achieved by effective antiangiogenic ability by the polyplex micelles with an optimal cross-linking degree, which enables the selective expression of loaded sFlt-1 gene in tumor tissue.

Experimental Section

Materials. pDNA for luciferase (Luc) with the pCAcc vector having the CAG promoter was provided by RIKEN Gene Bank (Tsukuba, Japan) and amplified in competent DH5α *Escherichia coli*, followed by purification using a NucleoBond Xtra Maxi (Machery-Nagel GmbH & Co. KG, Düren, Germany). Dulbecco's modified Eagle's medium (DMEM) and RPMI 1640 medium were purchased from Sigma-Aldrich Co. (Madison, WI). Fetal bovine serum (FBS) was purchased from Dainippon Sumitomo Pharma Co., Ltd. (Osaka, Japan). Alexa488- and Alexa647-conjugated secondary antibodies to rat IgG were obtained from Invitrogen Molecular Probes (Eugene, OR). Human soluble VEGF R1/

(1) Folkman, J. Tumor Angiogenesis: Therapeutic Implications. *N. Engl. J. Med.* **1971**, *285*, 1182–1186.
(2) Quesada, A. R.; Munoz-Chapuli, R.; Medina, M. A. Anti-angiogenic Drugs: from Bench to Clinical Trials. *Med. Res. Rev.* **2006**, *26*, 483–530.
(3) Shibuya, M.; Yamaguchi, S.; Yamane, A.; Ikeda, T.; Tojo, A.; Matsushime, H.; Sato, M. Nucleotide Sequence and Expression of a Novel Human Receptor-type Tyrosine Kinase Gene (flt) Closely Related to the Fms Family. *Oncogene* **1990**, *5*, 519–524.
(4) Kendall, R. L.; Thomas, K. A. Inhibition of Vascular Endothelial Cell Growth Factor Activity by an Endogenously Encoded Soluble Receptor. *Proc. Natl. Acad. Sci. U.S.A.* **1993**, *90*, 10705–10709.
(5) Kendall, R. L.; Wang, G.; Thomas, K. A. Identification of a Natural Soluble Forma of the Vascular Endothelial Growth Factor Receptor, FLT-1, and Its Heterodimerization with KDR. *Biochem. Biophys. Res. Commun.* **1996**, *226*, 324–428.
(6) Kong, H. L.; Hecht, D.; Song, W.; Kovesdi, I.; Hackett, N. R.; Yayon, A.; Crystal, R. G. Regional Suppression of Tumor Growth by In Vivo Transfer of a cDNA Encoding a Secreted form of the Extracellular Domain of the Flt-1 Vascular Endothelial Growth Factor Receptor. *Hum. Gene Ther.* **1998**, *9*, 823–833.
(7) Kuo, C. J.; Farnebo, F.; Yu, E. Y.; Christofferson, R.; Swearingen, R. A.; Charter, R.; von Recum, H. A.; Yuan, J.; Kamihara, J.; Flynn, E.; D' Amato, R.; Folkman, J.; Mulligan, R. C. Comparative Evaluation of the Antitumor Activity of Antiangiogenic Proteins Delivered by Gene Transfer. *Proc. Natl. Acad. Sci. U.S.A.* **2001**, *98*, 4605–4610.
(8) Kim, W. J.; Yockman, J. W.; Jeong, J. H.; Christensen, L. V.; Lee, M.; Kim, Y. H.; Kim, S. W. Anti-angiogenic Inhibition of Tumor Growth by Systemic Delivery of PEI-g-PEG-RGD/pCMV-sFlt-1 Complexes in Tumor-bearing Mice. *J. Controlled Release* **2006**, *114*, 381–388.
(9) Kommareddy, S.; Amiji, M. Antiangiogenic Gene Therapy with Systemically Administered sFlt-1 Plasmid DNA in Engineered Gelatin-based Nanovactors. *Cancer Gene Ther.* **2007**, *14*, 488–498.
(10) Miyata, K.; Kakizawa, Y.; Nishiyama, N.; Harada, A.; Yamasaki, Y.; Koyama, H.; Kataoka, K. Block Catiomer Polyplexes with Regulated Densities of Charge and Disulfide Cross-linking Directed to Enhance Gene Expression. *J. Am. Chem. Soc.* **2004**, *126*, 2355–2361.
(11) Miyata, K.; Kakizawa, Y.; Nishiyama, N.; Yamasaki, Y.; Watanabe, T.; Kohara, M.; Kataoka, K. Freeze-dried Formulations for *In Vivo* Gene Delivery of PEGylated Polyplex Micelles with Disulfide Crosslinked Cores to the Liver. *J. Controlled Release* **2005**, *109*, 15–23.
(12) Itaka, K.; Yamauchi, K.; Harada, A.; Nakamura, K.; Kawaguchi, H.; Kataoka, K. Polyion Complex Micelles from Plasmid DNA and Poly(ethylene glycol)-poly(L-lysine) Block Copolymer as Serum-tolerable Polyplex System: Physicochemical Properties of Micelles Relevant to Gene Transfection Efficiency. *Biomaterials* **2003**, *24*, 4495–4506.
(13) Kano, M. R.; Bae, Y.; Iwata, K.; Morishita, Y.; Yashiro, M.; Oka, M.; Fujii, T.; Komuro, A.; Kiyono, K.; Kaminishi, M.; Hirakawa, K.; Ouchi, Y.; Nishiyama, N.; Kataoka, K.; Miyazono, K. Improvement of Cancer-targeting Therapy, Using Nanocarriers for Intractable Solid Tumors by Inhibition of TGF-beta Signaling. *Proc. Natl. Acad. Sci. U.S.A.* **2007**, *104*, 3460–3465.

Flt-1 immunoassay kit was purchased from R&D Systems, Inc. (Minneapolis, MN). Gemcitabine was obtained from Eli Lilly and Company (Indianapolis, IN). Avastin was obtained from F. Hoffmann-La Roche, Ltd. (Basel, Switzerland). Synthesis of thiolated block copolymer, and construction and confirmation of pDNA encoding sFlt-1 are shown in the Supporting Information. A block copolymer with *X*% of thiolation degree was abbreviated as "B-SH*X*%".

Cell Lines and Animals. Human embryonic kidney 293T cells (from RIKEN CELL BANK, Tsukuba, Japan) and human pancreatic adenocarcinoma BxPC3 cells (from ATCC, Manassas, VA) were maintained in DMEM and RPMI medium, respectively, supplemented with 10% FBS in a humidified atmosphere containing 5% CO_2 at 37 °C. 293T cells were chosen for *in vitro* experiments as cells that did not express sFlt-1.[14] Balb/c nude mice (female, 5 weeks old) were purchased from Charles River Laboratories (Tokyo, Japan). All animal experimental protocols were performed in accordance with the Guide for the Care and Use of Laboratory Animals as stated by the National Institutes of Health.

Preparation of Polyplex Micelles. Each block copolymer was dissolved in 10 mM Tris-HCl buffer (pH 7.4), followed by the addition of 10-times-excess mol of dithiothreitol (DTT) against thiol groups. After 30 min incubation at room temperature, the polymer solution was added to a twice-excess volume of 225 μg/mL pDNA/10 mM Tris-HCl (pH 7.4) solution to form polyplex micelles with N/P ratio = 2. Note that N/P ratio was defined as the residual molar ratio of amino groups of thiolated PEG-PLys to phosphate groups of pDNA. The final pDNA concentration was adjusted to 150 μg/mL. After overnight incubation at room temperature, the polyplex micelle solution was dialyzed against 10 mM Tris-HCl buffer (pH 7.4) containing 0.5 vol% DMSO at 37 °C for 24 h to remove the impurities, followed by 24 h of additional dialysis against 10 mM Tris-HCl buffer (pH 7.4) or 10 mM Hepes buffer (pH 7.4) to remove DMSO. During the dialysis, the thiol groups of thiolated block copolymers were oxidized to form disulfide cross-links. In the *in vivo* experiments, the polyplex micelle solution was adjusted to a concentration of 100 μg of pDNA/mL in 10 mM Hepes buffer (pH 7.4) with 150 mM NaCl.

Dynamic Light Scattering (DLS) Measurement. The size of the polyplex micelles was evaluated by DLS using Nano ZS (ZEN3600, Malvern Instruments, Ltd., U.K.). A He−Ne ion laser (633 nm) was used as the incident beam. Polyplex micelle solutions with N/P = 2 from 3 different batches were adjusted to a concentration of 33.3 μg of pDNA/mL in 10 mM Tris-HCl buffer (pH 7.4). The data obtained at a detection angle of 173° and a temperature of 37 °C were analyzed by a cumulant method to obtain the hydrodynamic diameters and polydispersity indices (μ/Γ^2) of micelles.

Zeta-Potential Measurement. The zeta-potential of polyplex micelles was evaluated by the laser-Doppler electrophoresis method using Nano ZS with a He−Ne ion laser (633 nm). Polyplex micelle solutions with N/P = 2 from 3 different batches were adjusted to a concentration of 33.3 μg pDNA/mL in 10 mM Tris-HCl buffer (pH 7.4). The zeta-potential measurements were carried out at 37 °C. A scattering angle of 173 °C was used in these measurements.

Real-Time Gene Expression. 293T cells (100,000 cells) were seeded on a 35 mm dish and incubated overnight. After replacement with fresh medium containing 0.1 mM D-luciferin, each type of polyplex micelle (N/P = 2) containing 3 μg of Luc pDNA was added. The dishes were set in a luminometer incorporated in a CO_2 incubator (AB-2550 Kronos Dio, ATTO, Tokyo, Japan), and the bioluminescence was monitored every 10 min with an exposure time of 1 min. Reproducibility was confirmed by triplicate experiments.

Antitumor Activity Assay. Balb/c nude mice were inoculated subcutaneously with BxPC3 cells (5×10^6 cells in 100 μL of PBS). Tumors were allowed to grow for 2−3 weeks to reach the proliferative phase (the size of the tumors at this point was approximately 60 mm^3). Subsequently, polyplex micelles (20 μg of pDNA/mouse), gemcitabine (100 mg/kg), or Avastin (50 mg/kg) maintained in 10 mM Hepes buffer (pH 7.4) with 150 mM NaCl were injected via the tail vein either 3 times (Figure 2a) or 5 times (Figure 2b) at 4-day intervals. Gemcitabine and Avastin doses and injection regimens were according to the previous reports published elsewhere.[15,16] A polyplex micelle containing Luc pDNA was used as a control formulation containing the nontherapeutic gene. Tumor size was measured every second day by a digital vernier caliper across its longest (*a*) and shortest diameters (*b*), and its volume (*V*) was calculated according to the formula $V = 0.5ab^2$.

***In Vivo* sFlt-1 Gene Expression.** Polyplex micelles loading either sFlt-1 or Luc pDNA (20 μg pDNA) were injected into the BxPC3-inoculated mice via the tail vein on days 0 and 4. Mice were sacrificed on day 6 after collecting blood, and the lungs, livers, spleens, kidneys, and tumors were excised. The excised organs were treated in 500 μL of cell culture lysis buffer (Promega, Madison, WI), homogenized, and centrifuged. The sFlt-1 concentration of supernatants was evaluated using the immunoassay kit according to the manufacturer's protocol. Note that block copolymers and polyplex micelles did not interfere with ELISA (Figure 2 in the Supporting Information).

Vascular Density in the Tumors. Polyplex micelles loading either sFlt-1 or Luc pDNA (20 μg of pDNA) and Avastin (50 mg/kg) were injected into the BxPC3-inoculated

(14) Kim, W. J.; Yockman, J. W.; Lee, M.; Jeong, J. H.; Kim, Y. H.; Kim, S. W. Soluble Flt-1 Gene Delivery Using PEI-g-PEG-RGD Conjugate for Anti-angiogenesis. *J. Controlled Release* **2005**, *106*, 224–234.

(15) Braakhuis, B. J. M.; van Dongen, G. A. M. S.; Vermorken, J. B.; Snow, G. B. Preclinical In Vivo Activity 2′,2′-Difluorodeoxycytidine (Gemcitabine) against Human Head and Neck Cancer. *Cancer Res.* **1991**, *51*, 211–214.

(16) Gerber, H. P.; Ferrara, N. Pharmacology and Pharmacodynamics of Bevacizumab as Monotherapy or in Combination with Cytotoxic Therapy in Preclinical Studies. *Cancer Res.* **2005**, *65*, 671–680.

mice via the tail vein on days 0 and 4. Mice were sacrificed on day 6, and the tumors were excised, frozen in dry-iced acetone, and sectioned at 10 μm thickness in a cryostat. Vascular endothelial cells (VECs) were immunostained by rat monoclonal antibody antiplatelet endothelial cell adhesion molecule-1 (PECAM-1) (BD Pharmingen, Franklin Lakes, NJ) and Alexa488-conjugated secondary antibody. The samples were observed with a confocal laser scanning microscope (CLSM). The CLSM observation was performed using an LSM 510 (Carl Zeiss, Oberlochen, Germany) with an EC Plan-Neoflur 20× objective (Carl Zeiss) at the excitation wavelength of 488 nm (Ar laser). The PECAM-1-positive area (%) was calculated from Alexa488-positive pixels.

***In Vivo* EGFP Gene Expression in the Tumors.** Polyplex micelles loading EGFP pDNA (20 μg of pDNA) were injected into the BxPC3-inoculated mice via the tail vein. Mice were sacrificed on either day 3 or day 7. Tumors were excised, fixed with 10% formalin, frozen, and sectioned. VECs were immunostained by anti-PECAM-1 antibody and Alexa647-conjugated secondary antibody. After nuclear staining with Hoechst 33342, CLSM observation was carried out using the LSM 510 with the EC Plan-Neoflur 20× objective at the excitation wavelength of 488 nm for EGFP expression, 633 nm (He−Ne laser) for Alexa647, and 710 nm (MaiTai laser, two photon excitation; Spectra-Physics, Mountain View, CA) for Hoechst 33342, respectively. The representative images of tumors excised on day 3 are shown in Figure 5. Note that images of tumors excised on day 7 showed similar patterns to those on day 3, however with lower intensity of EGFP expression.

Results

Formation of Polyplex Micelles. No free pDNA was detected by agarose gel electrophoresis, confirming that all pDNA was entrapped in disulfide cross-linked polyplex micelles, which were prepared as previously reported through ion complexation of block copolymers with pDNA at the N/P ratio = 2. Free thiol groups in polyplex micelles were estimated to be less than 2% by Ellman's test (data not shown), which is consistent with our previous report.[10] Weight−weight % ratios of pDNA/micelle in each formulation were as follows: 32.8% in B-SH0% formulation; 31.0% in B-SH5%; 29.2% in B-SH11%; 26.4% in B-SH20%; and 21.0% in B-SH36%. The mean size of the micelles was between 100 and 150 nm, with a moderate polydispersity index between 0.17 and 0.2 (Figure 3 in the Supporting Information), while zeta-potential revealed approximately neutral values, confirming the formation of PEG palisade surrounding the polyplex core (Table 1).

Real-Time Gene Expression. *In vitro* real-time Luc gene expression of polyplex micelles was evaluated using Kronos

Table 1. Sizes and Zeta-Potentials of Polyplex Micelles with Various Cross-Linking Rates at N/P = 2[a]

thiolation degree (%)	cumulant diameter (nm)	polydispersity index (μ/Γ^2)	zeta-potential (mV)
0	107 ± 2	0.195 ± 0.021	1.66 ± 0.28
5	117 ± 2	0.184 ± 0.011	1.25 ± 0.40
11	116 ± 2	0.171 ± 0.013	1.02 ± 0.30
20	139 ± 6	0.182 ± 0.050	0.40 ± 0.07
36	147 ± 2	0.192 ± 0.061	−0.96 ± 0.02

[a] The results reported were expressed as mean ± SEM (n = 3).

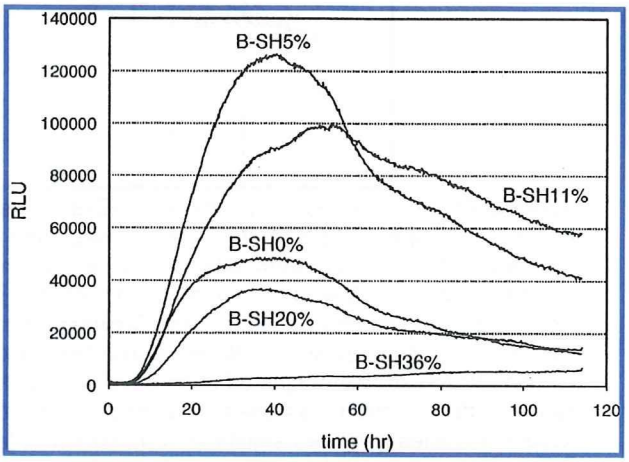

Figure 1. Real-time luciferase gene expression of the polyplex micelles with varying thiolation degrees at N/P = 2 against 293T cells.

Dio for a prolonged period (Figure 1).[17,18] The B-SH5% cross-linked polyplex micelle showed the highest gene expression among all micelles until 60 h. Worth mentioning is that the transfection efficiency of the B-SH11% micelle continued to exceed that of the B-SH5% micelle after 60 h. Disulfide cross-links in the polyplex core are believed to contribute not only to enhanced stability of the micelles in the medium but also to sustained release of complexed pDNA inside the cells with a reductive environment, resulting in polyplex micelles with higher cross-linking rates that can maintain an appreciable transfection efficiency over a longer time scale. Note that the B-SH36% micelle showed an increasing trend in gene expression with time.

Antitumor Activity. Polyplex micelles containing sFlt-1 pDNA were injected iv into mice bearing pancreatic adenocarcinoma BxPC3, followed by evaluation of tumor volume (Figure 2). All the micelles were injected three times on days

(17) Takae, S.; Miyata, K.; Oba, M.; Ishii, T.; Nishiyama, N.; Itaka, K.; Yamasaki, Y.; Koyama, H.; Kataoka, K. PEG-detachable Polyplex Micelles Based on Disulfide-crosslinked Block Cationers as Bioresponsive Nonviral Gene Vectors. *J. Am. Chem. Soc.* **2008**, *130*, 6001–6009.

(18) Oba, M.; Aoyagi, K.; Miyata, K.; Matsumoto, Y.; Itaka, K.; Nishiyama, N.; Yamasaki, Y.; Koyama, H.; Kataoka, K. Polyplex Micelles with Cyclic RGD Peptide Ligands and Disulfide Cross-links Directing to the Enhanced Transfection via Controlled Intracellular Trafficking. *Mol. Pharmaceutics* **2008**, *5*, 1080–1092.

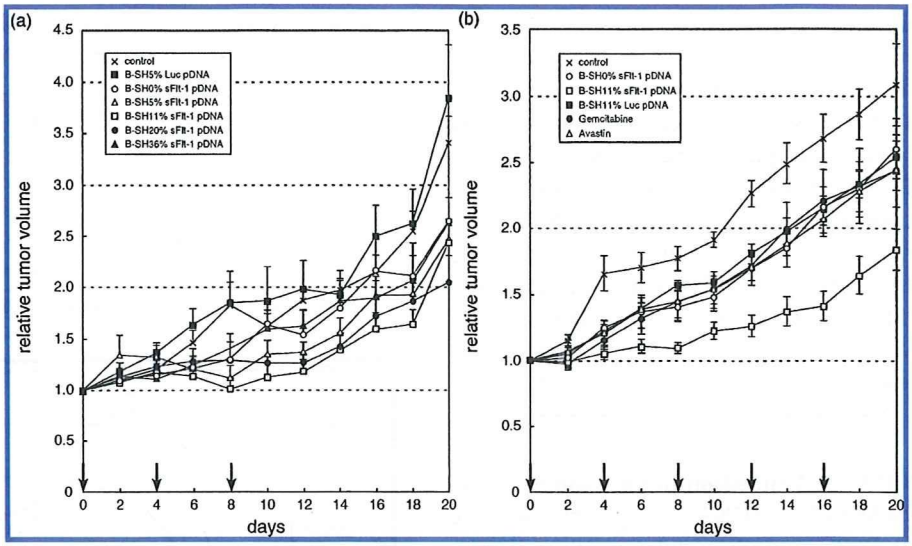

Figure 2. Antitumor activity of polyplex micelles with sFlt-1 pDNA in subcutaneously BxPC3-inoculated mice. (a) Effect of thiolation degree. Hepes buffer (control) was used as a negative control. Polyplex micelles were injected iv on days 0, 4, and 8 at 20 μg pDNA/mouse, and mice were monitored for the relative tumor volume every second day. Error bars represent the SEM ($n = 6$). Only the B-SH11% polyplex micelles exhibited significant retardation of tumor growth compared to the control ($P < 0.01$). (b) Growth curve study with an increased dose of the B-SH11% polyplex micelles compared to commercially available drugs. Polyplex micelles (20 μg pDNA/mouse), gemcitabine (100 mg/kg), and Avastin (50 mg/kg) were injected iv on days 0, 4, 8, 12, and 16. Relative tumor size was measured every second day. Hepes buffer (control) was used as a negative control. Error bars represent the SEM ($n = 5$). Only the B-SH11% polyplex micelles exhibited significant retardation of tumor growth compared to the control ($P < 0.001$). P values were calculated by multivariate ANOVA study.

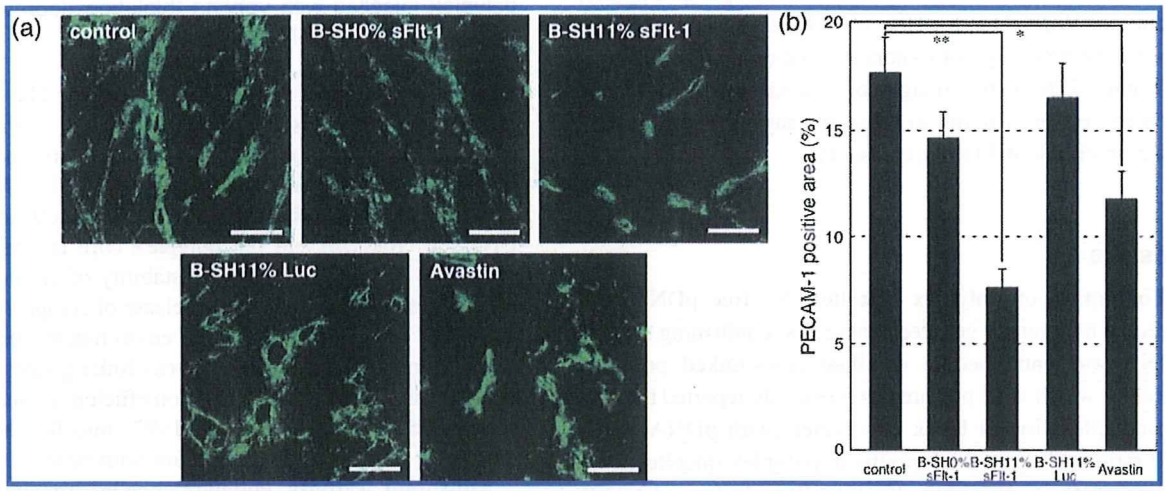

Figure 3. Immunostaining of the VECs in the BxPC3 tumor tissue by PECAM-1 antibody. Hepes buffer (control), three types of polyplex micelles (20 μg of pDNA/mouse), and Avastin (50 mg/kg) were injected into the BxPC3-inoculated mice via the tail vein on days 0 and 4. Mice were sacrificed on day 6, and tumors were excised and immunostained. (a) CLSM images of immunostained tumors. PECAM-1-positive regions are green. Bars represent 100 μm. (b) Areas of PECM-1-positive endothelium were quantified. Error bars represent the SEM ($n = 15$). P values were calculated by Student's t test. $^*P < 0.01$ and $^{**}P < 0.001$.

0, 4, and 8 (Figure 2a). The B-SH11% micelle significantly suppressed tumor growth compared to control mice treated with Hepes buffer ($P < 0.01$). There was no significant change in tumor growth after injection of other polyplex micelles, implying that an optimal cross-linking rate is required to achieve an effective expression of the gene. Encouraged by these results, the tumor growth suppression activity of B-SH11% micelle was further evaluated, implying a regimen with enhanced number of injections. The effect of the micelles was compared to commercially available drugs, gemcitabine, a standard chemotherapeutic agent for pancreatic tumor, and bevacizumab (Avastin), a monoclonal antibody against VEGF (Figure 2b). The doses of gemcitabine and Avastin implied in our study were based on

previous reports published elsewhere.[15,16] The administration of B-SH11%/sFlt-1 micelle resulted in significant suppression of tumor growth ($P < 0.001$), while gemcitabine and Avastin, under the reported experimental regimen, showed no remarkable therapeutic effect. Note that the difference observed in tumor volumes between the B-SH11%/Luc micelle-treated group and the control group was not significant.

Tumor Vascular Density. The antiangiogenic effect of expressed sFlt-1 was confirmed by immunostaining of VECs using PECAM-1 (Figure 3). Vascular density of tumors treated with either B-SH11%/sFlt-1 micelle or Avastin was significantly lower than that of the other groups. The most pronounced and significant effect on neo-vasculature suppression was achieved by B-SH11%/sFlt-1 micelle (7% PECAM-1 positive area) over Avastin (12% PECAM-1 positive area) ($P < 0.05$). These results suggest that the expressed sFlt-1 may entrap VEGF secreted in the tumor tissue, thereby suppressing the growth of VECs.

***In Vivo* sFlt-1 Gene Expression.** Expression levels of sFlt-1 in the body were then evaluated by measuring the amount of sFlt-1 in lung, liver, spleen, kidney, tumor, and blood plasma using enzyme-linked immunosorbent assay (ELISA) (Figure 4). Injection of B-SH11%/sFlt-1 micelle resulted in significantly higher expression of sFlt-1 selectively in tumor tissue compared to the control. On the other hand, injection of B-SH0%/sFlt-1 micelle or B-SH11%/Luc micelle did not result in any difference in sFlt-1 expression compared to the control. These results strongly support that tumor-specific elevation in sFlt-1 expression led to the significant growth suppression of VECs in the tumor tissue and, eventually, the suppression of tumor growth.

***In Vivo* Enhanced Green Fluorescence Protein (EGFP) Gene Expression in Tumors.** The location of gene expression in BxPC3 tumors after administration of the micelles was analyzed histologically using pDNA encoding EGFP (Figure 5). As previously reported,[13,19,20] thick fibrotic tissue was formed around blood vessels (red) inside the stroma of BxPC3 tumors, and nests of tumor cells (region T) were scattered in the stroma (Figure 5a). The expression of EGFP (Figures 5b and 5c) was observed mainly in the VECs and cells in stromal regions adjacent to some vasculature, indicating that VECs and fibroblasts near some vasculature in the stroma, but not the tumor cells, were transfected. As seen in Figure 5a, there were thick fibrotic tissues around blood vessels in the BxPC3 xenograft,

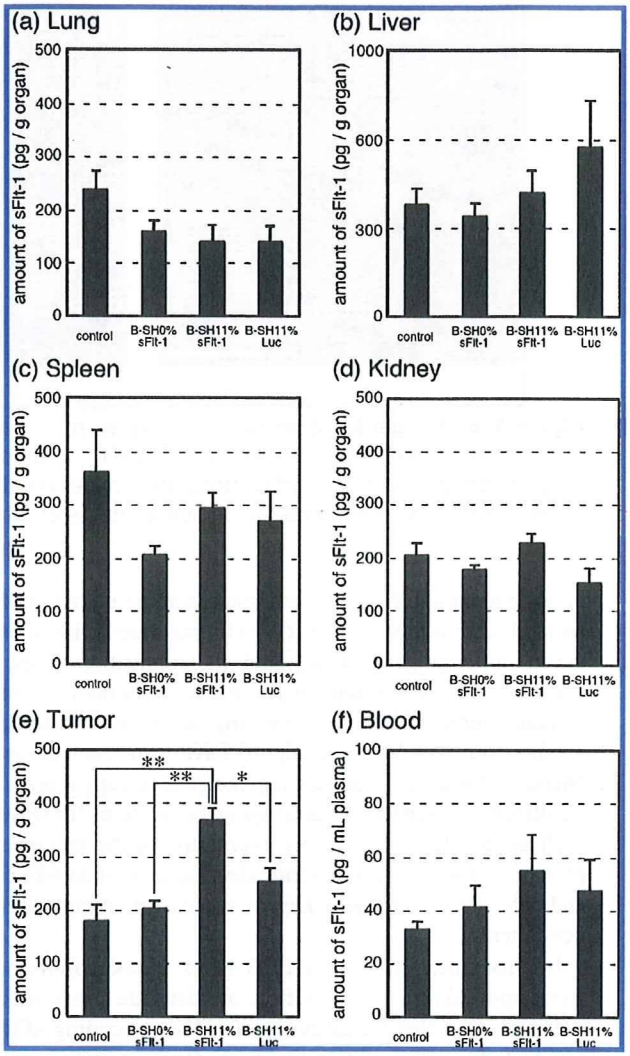

Figure 4. Evaluation of sFlt-1 gene expression in organs by ELISA. Hepes buffer (control) and three types of polyplex micelles (20 μg pDNA/mouse) were injected into the BxPC3-inoculated mice via the tail vein on days 0 and 4. Mice were sacrificed on day 6 after collecting blood (f), and the lungs (a), livers (b), spleens (c), kidneys (d), and tumors (e) were excised, followed by evaluation of sFlt-1 concentration by ELISA according to the manufacturer's protocol. Error bars represent the SEM ($n = 6$). P values were calculated by Student's t test. $^*P < 0.01$ and $^{**}P < 0.001$.

indicating that the penetration of polyplex micelles deep into the stroma or into the tumor nest was interrupted and the gene expression was limited in the VECs and some of the fibroblasts in the stroma. Higher levels of EGFP expression were observed for B-SH11% micelle, confirming their enhanced ability to accumulate inside tumor tissue compared to B-SH0% micelle.

Discussion

Since all solid tumors need angiogenesis for their growth, antiangiogenic therapy is a promising strategy for treating

(19) Miyata, K.; Oba, M.; Kano, M. R.; Fukushima, S.; Vachutinsky, Y.; Han, M.; Koyama, H.; Miyazono, K.; Nishiyama, N.; Kataoka, K. Polyplex Micelles from Triblock Copolymers Composed of Tandemly Aligned Segments with Biocompatible, Endosomal Escaping, and DNA-condensing Functions for Systemic Gene Delivery to Pancreatic Tumor Tissue. *Pharm. Res.* **2008**, *25*, 2924–2936.

(20) Kano, M. R.; Komuta, Y.; Iwata, K.; Oka, M.; Shirai, Y.; Morishita, Y.; Ouchi, Y.; Kataoka, K.; Miyazono, K. Comparison of the Effects of the Kinase Inhibitors Imatinib, Sorafenib, and Transforming Growth Factor-β Receptor Inhibitor on Extravasation of Nanoparticles from Neovasculature. *Cancer Sci.* **2009**, *100*, 173–180.

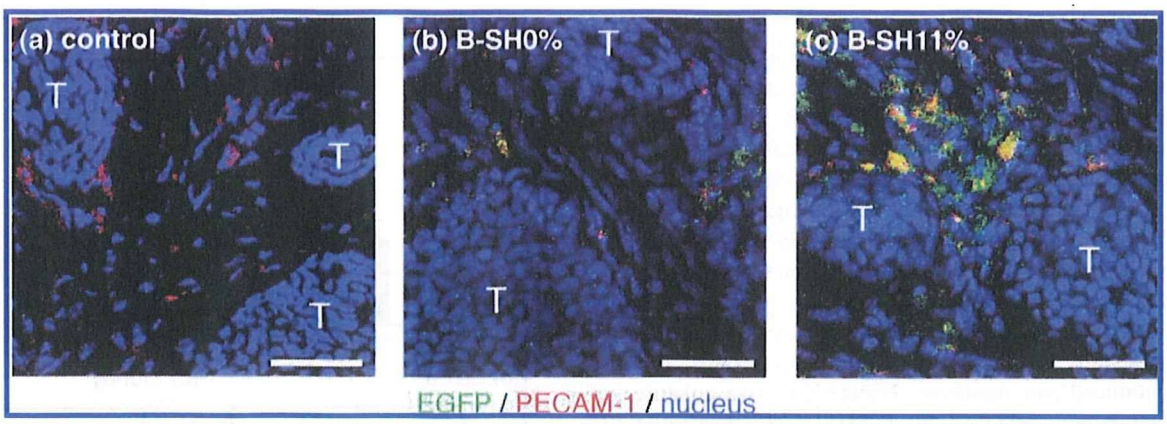

Figure 5. EGFP gene expression by polyplex micelles in the inoculated BxPC3 tumors. Hepes buffer (a) was used as a negative control. B-SH0% (b) and B-SH11% (c) polyplex micelles containing EGFP pDNA (20 μg pDNA/mouse) were injected into the BxPC3-inoculated mice via the tail vein. Mice were sacrificed on day 3, and tumors were excised and immunostained. "T" indicates nests of tumor cells in tumor tissues. Bars represent 50 μm.

tumor patients. In fact, Avastin, the recombinant humanized monoclonal antibody against VEGF, has been widely used as an antiangiogenic drug, and its application range is spreading to the various types of solid tumors.[16] Other antiangiogenic proteins,[21,22] e.g., angiostatin, endostatin, and soluble forms of VEGF receptor, have also received great attention. Meanwhile, antiangiogenic gene therapy represents an attractive alternative to antiangiogenic proteins for reasons such as low dose, continuous expression of the therapeutic protein, and low cost. Therefore, development of an effective and safe gene vector is a key to successful antiangiogenic gene therapy.

In this study, thiolated PEG-PLys block copolymers were applied in the formation of disulfide cross-linked polyplex micelles for delivery of pDNA encoding sFlt-1, and tested for their antiangiogenic effect on mice bearing xenografted BxPC3 cell line, derived from human pancreatic adenocarcinoma. Disulfide cross-links in the polyplex core were designed to increase blood stability of the polyplex micelles and effectively release pDNA in the intracellular milieu.[10,11,18] PEG palisade of the polyplex micelle is expected to cover the polyplex core to shield the positive charge as well as to decrease interfacial free energy.[12,23] The formation of the PEG palisade surrounding the polyplex core was confirmed by the neutral zeta-potential of the polyplex micelles (Table 1). B-SH36% micelle showed an approximately 10 times higher concentration of pDNA in the blood at 60 min after iv injection than that of the micelle without core cross-linking (B-SH0%) (Figure 4 in the Supporting Information). The disulfide cross-links in the polyplex core apparently contribute to the enhanced stability of the micelles in the bloodstream. Note that the size of polyplex micelles is between 100 and 150 nm (Table 1), which may be in a suitable range for accumulation in solid tumors due to the enhanced permeability and retention (EPR) effect,[24] although the size may be too large to allow the micelles to penetrate into the stroma in pancreatic tumors.[13] Nevertheless, there is a concern that excessive disulfide cross-links interfere with the smooth release of entrapped pDNA in the core, resulting in decreased transfection efficiency.[10] Accordingly, optimal cross-linking density should be determined to balance the stability and maintain high transfection efficiency. The results of *in vitro* real-time gene expression showed that B-SH5% micelle possessed the highest efficiency among the evaluated samples up to 60 h after transfection. It is noteworthy that B-SH11% micelle exerted sustained Luc expression and kept an appreciably high efficiency beyond 60 h (Figure 1). Apparently, gene expression is prolonged with an increase in cross-linking rates, although excess cross-links induced overstabilization of polyplex micelles, resulting in decreased transfection efficiency in the case of the B-SH20% and B-SH36% micelles. Eventually, the B-SH36%/sFlt-1 micelle had no *in vivo* efficiency, even though they showed the highest stability in the bloodstream among the evaluated samples (Figure 4 in the Supporting Information). It is also noteworthy that the B-SH11%/sFlt-1 micelle achieved an appreciably high therapeutic efficiency, even though it showed only limited improvement in blood circulation time compared to the B-SH0% and B-SH5% systems. Presumably, a sustained

(21) Sim, B. K. L.; MacDonald, N. J.; Gubish, E. R. Angiostatin and Endostatin: Endogenous Inhibitors of Tumor Growth. *Cancer Metastasis Rev.* **2000**, *19*, 181–190.
(22) Fischer, C.; Mazzone, M.; Jonckx, B.; Carmeliet, P. FLT1 and Its Ligands VEGFB and PIGF: Drug Targets for Anti-angiogenic Therapy. *Nat. Rev. Cancer* **2008**, *8*, 942–956.
(23) Kakizawa, Y.; Kataoka, K. Block Copolymer Micelles for Delivery of Gene and Related Compounds. *Adv. Drug Delivery Rev.* **2002**, *54*, 203–222.
(24) Matsumura, Y.; Maeda, H. A New Concept for Macromolecular Therapeutics in Cancer Chemotherapy: Mechanism of Tumoritropic Accumulation of Proteins and the Antitumor Agent Smancs. *Cancer Res.* **1986**, *46*, 6387–6392.

profile in gene expression may have been the key to this achievement. Note that no change in body weight of the mice was observed during the experiment (data not shown), indicating few serious side effects of polyplex micelles.

Comparison with the commercially available agents, gemcitabine and Avastin, confirmed the encouraging tumor growth suppression effect of the B-SH11% polyplex micelle (Figure 2b). Gemcitabine continues to be the standard therapy in the treatment of pancreatic tumors; however, its objective response rate is limited in patients with advanced disease.[25] Avastin is a recombinant humanized monoclonal antibody against human VEGF, which may neutralize tumor-cell-derived VEGF in the model used here. In humans, Avastin is the first clinically available antiangiogenic drug, and it has been efficient when used in combined chemotherapy for metastatic colorectal cancer[26] and non-small-cell lung cancer.[27] However, it showed no benefit in patients with pancreatic tumors.[25] The B-SH11%/sFlt-1 micelle significantly suppressed tumor growth compared not only to the control ($P < 0.001$) but also to the B-SH11%/Luc micelle, gemcitabine, and Avastin ($P < 0.01$) (Figure 2b). Xenografted BxPC3 was reported not to respond to gemcitabine,[28] probably due to its inability to penetrate through the tumor thick fibrotic tissue and target tumor cells, which is consistent with our results. Evaluation of vascular density in BxPC3 tumor (Figure 3) clearly showed that the B-SH11%/sFlt-1 micelle decreased vascular density compared to the control ($P < 0.001$), the B-SH11%/Luc micelle ($P < 0.001$), and Avastin ($P < 0.05$) treated tumors.

Inhibitory effect on tumor growth (Figure 2) is consistent with the result of decreased vascular density. There are several studies on antiangiogenic gene therapy for subcutaneously inoculated tumors in mice by systemic expression of sFlt-1 using viral vectors, including im injection of adeno-associated viral vectors[29] and iv injection of adenoviral vectors to target livers.[30] In these studies, however, sFlt-1 was expressed mainly in organs rather than tumor tissue. What was worse, the excess expression of sFlt-1 in the liver led to unacceptable hepatotoxicity.[31] Thus, tumor-specific expression of sFlt-1 is essential for a safe and efficient antiangiogenic gene therapy. However, any nonviral gene vectors loading sFlt-1 gene have failed to exhibit selective gene expression in the tumor tissue, although they achieved certain inhibition of tumor growth.[8,9] In this regard, the B-SH11%/sFlt-1 micelle system might be promising, since sFlt-1 expression was significantly increased selectively in the tumor tissue compared not only to the control ($P < 0.001$) but also to the B-SH11%/Luc micelle ($P < 0.01$), as shown in Figure 4, without any significantly enhanced expression in other normal tissues. Note that no significant increase of sFlt-1 expression was observed in any normal organs treated with B-SH0%/sFlt-1 micelle or B-SH11%/Luc micelle. Histological analyses revealed that EGFP expression of the B-SH11%/EGFP micelle was located mainly around VECs but not in the tumor cells (Figure 5), probably due to restricted permeation of micelles by thick fibrotic tissues and pericyte-covered vasculature of the BxPC3 tumors. These results suggested the ability of expressed sFlt-1 molecule to entrap excess VEGF in the tumor tissue and to inhibit tumor growth by an antiangiogenic effect. Xenografted BxPC3 tumors in mice are characterized by stroma-rich histology,[20] which might explain the only slight inhibitory effects on BxPC3 growth achieved by gemecitabine[28] targeting tumor cells.

Conclusions

In conclusion, antiangiogenic gene therapeutic study was carried out by iv administration of polyplex micelles with sFlt-1 pDNA to mice bearing pancreatic adenocarcinoma BxPC3 xenografts, and the results demonstrated the ability of B-SH11% sFlt-1 micelle as a safe and effective gene delivery system. The optimal disulfide cross-linking rate of polyplex micelles was found to show significant suppression of tumor growth. Gene expression of sFlt-1 by iv injection of polyplex micelles was observed in tumor tissue only, followed by decreased vascular density and significant suppression of tumor growth. Based on these results, the B-SH11% disulfide cross-linked polyplex

(25) Rocha-Lima, C. M. New Directions in the Management of Advanced Pancreatic Cancer: a Review. *Anti-Cancer Drugs* **2008**, *19*, 435–446.

(26) Hurwitz, H.; Fehrenbacher, L.; Novotny, W.; Cartwright, T.; Hainsworth, J.; Heim, W.; Berlin, J.; Baron, A.; Griffing, S.; Holmgren, E.; Ferrara, N.; Fyfe, G.; Rogers, B.; Ross, R.; Kabbinavar, F. Bevacizumab Plus Irinotecan, Fluorouracil, and Leucovorin for Metastatic Colorectal Cancer. *N. Engl. J. Med.* **2004**, *350*, 2335–2342.

(27) Sandler, A.; Gray, R.; Perry, M. C.; Brahmer, J.; Schiller, J. H.; Dowlati, A.; Lilenbaum, R.; Johnson, D. H. Paclitaxel-carboplatin Alone or with Bevacizumab for Non-small-cell Lung Cancer. *N. Engl. J. Med.* **2006**, *355*, 2542–2550.

(28) Merriman, R. L.; Hertel, L. W.; Schultz, R. M.; Houghton, P. J.; Houghton, J. A.; Rutherford, P. G.; Tanzer, L. R.; Boder, G. B.; Grindey, G. B. Comparison of the Antitumor Activity of Gemcitabine and Ara-C in a Panel of Human Breast, Colon, Lung and Pancreatic Xenograft Models. *Invest. New Drugs* **1996**, *14*, 243–247.

(29) Takei, Y.; Mizukami, H.; Saga, Y.; Yoshimura, I.; Hasumi, Y.; Takayama, T.; Kohno, T.; Matsushita, T.; Okada, T.; Kume, A.; Suzuki, M.; Ozawa, K. Suppression of Ovarian Cancer by Muscle-Mediated Expression of Soluble VEGFR-1/Flt-1 Using Adeno-associated Virus Serotype 1-derived Vector. *Int. J. Cancer* **2006**, *120*, 278–284.

(30) Liu, J.; Li, J.; Su, C.; Huang, B.; Luo, S. Soluble Fms-like Tyrosine Kinase-1 Expression Inhibits the Growth of Multiple Myeloma in Nude Mice. *Acta Biochim. Biophys. Sin.* **2007**, *39*, 499–506.

(31) Mahasreshti, P. J.; Kataram, M.; Wang, M. H.; Stockard, C. R.; Grizzle, W. E.; Carey, D.; Siegal, G. P.; Haisma, H. J.; Alvarez, R. D.; Curiel, D. T. Intravenous Delivery of Adenovirus-mediated Soluble FLT-1 Results in Liver Toxicity. *Clin. Cancer Res.* **2003**, *9*, 2701–2710.

micelle with sFlt-1 pDNA is interesting and worthy to develop further for antiangiogenic gene therapy of solid tumors.

Acknowledgment. This work was financially supported in part by the Core Research Program for Evolutional Science and Technology (CREST) from Japan Science and Technology Agency (JST) as well as by Grants-in-Aid for Young Scientists (A) and Exploratory Research. We express our appreciation to Masabumi Shibuya (Tokyo Medical and Dental University) for providing pVL 1393 baculovirus vector pDNA encoding human sFlt-1. We thank Kazuhiro Aoyagi, Yoko Hasegawa, Kotoe Date, and Satomi Ogura (The University of Tokyo) for technical assistance.

Supporting Information Available: Synthesis of thiolated block copolymer and Supporting Figures 1, 2, 3, and 4. This material is available free of charge via the Internet at http://pubs.acs.org.

MP9002317

Versatile and Selective Synthesis of "Click Chemistry" Compatible Heterobifunctional Poly(ethylene glycol)s Possessing Azide and Alkyne Functionalities

Shigehiro Hiki[†] and Kazunori Kataoka*[,†,‡,§]

Department of Materials Engineering, Graduate School of Engineering, and Center for NanoBio Integration, The University of Tokyo, 7-3-1 Hongo, Bunkyo-ku, Tokyo 113-8656, Japan, Core Research Program for Evolutional Science and Technology (CREST), Japan Science and Technology Agency (JST), Tokyo, Japan, and Center for Disease Biology and Integrative Medicine, Graduate School of Medicine, The University of Tokyo, 7-3-1 Hongo, Bunkyo-ku, Tokyo 113-0033, Japan.
Received June 16, 2009; Revised Manuscript Received December 9, 2009

Versatile route for "click chemistry" compatible heterobifunctional PEGs was established through preparation of α-tetrahydropyranyloxy-ω-hydroxyl poly(ethylene glycol) (THP-PEG-OH) via ring-opening polymerization of ethylene oxide using 2-(tetrahydro-2*H*-pyran-2-yloxy)ethanol as an initiator, followed by the functionalization of ω-OH group to either the azido or alkyne group. Quantitative azidation of THP-PEG-OH was confirmed from the analysis of molecular functionality of the derivatives. While the conversion efficiency of ω-alkynation was appropriately 70%, the unreacted THP-PEG-OH fraction was successfully removed by ion-exchange chromatography after the carboxylation of the hydroxyl group with succinic anhydride. Then, the protecting group of the α-end, THP, was removed in mild acidic media, followed by two- or three-step modification of the resulting α-hydroxyl group to primary amino or thiol groups. Consequently, "click chemistry" compatible heterobifunctional PEG derivatives (X-PEG-Y; X = NH_2 and SH, Y =Azide and Alkyne) were synthesized with high efficiency and controlled molecular weight.

INTRODUCTION

Conjugation and immobilization of biomolecules (e.g., proteins, peptides, and carbohydrates) with functional small molecules and synthetic polymers have widely been used as a useful research tool in chemical, biological, and pharmaceutical fields. The former group mainly consists of fluorescence reagents such as organic dyes, which were exploited for target detection and quantification (*1, 2*). The latter has been aimed at alteration or improvement of the physicochemical properties of biomacromolecules. The most successful strategy employs poly(ethylene glycol) (PEG) as the conjugating polymer, termed "PEGylation" (*3*−*5*). In general, PEGylation improves water solubility, reduces toxicity, and increases the tolerance against enzymatic degradation and the in vivo half-lives of bioactive macromolecules (*3*−*6*). Indeed, several PEGylated therapeutic proteins have clinically been investigated (*7, 8*).

The Cu(I)-catalyzed 1,3-dipolar cycloaddition of azides and terminal alkynes to form a triazole ring, "click chemistry" coined by Sharpless, has recently received considerable attention (*9*−*11*) and been utilized as a versatile ligation reaction in the field of bioconjugation including PEGylation (*12, 13*). This "click" reaction is highly chemoselective and can be performed under mild conditions in aqueous buffers with a wide range of pH, indicating high applicability for site-specific conjugation. Therefore, the PEGylation technique integrated with "click chemistry" is a promising approach for site-specific modification of bioactive macromolecules (*14, 15*). Indeed, there are several reports including the "click"-based PEGylation procedure for the preparation of well-defined polymers and functional nanostructures, demonstrating the efficient reaction with high conversion in aqueous condition as well as in organic solvents (*16*−*18*). Additionally, to construct PEGylated biopharmaceutics with multifunctionality, development of α,ω-heterobifunctional PEGs with both well-controlled molecular weight and high derivatizability is inevitable. Although preparation of heterobifunctional PEG having an azido or alkyne group at one end may be feasible using of homobifunctional PEGs as the starting materials, the synthetic methods contain some drawbacks such as repeated column purification in each reaction step and, consequently, low yield. Thus, exploiting of versatile synthetic design of α,ω-heterobifunctional PEGs with high productivity and compatibility to "click"-based conjugation is essential.

In a previous paper, we reported the preparation of azido-terminated heterobifunctional PEGs using a radical addition of thiol compounds to the allyl terminus of PEG derivative (*19*). This radical addition method, however, is inadaptable to the utilization of the alkyne moiety. Herein, we wish to communicate the facile synthetic route applicable to heterobifunctional PEGs possessing azido or alkyne function at one chain end with controlled molecular weight via the ring-opening polymerization of ethylene oxide. Monoprotected ethylene glycol derivative, which was obtained by tetrahydropyranylation of one hydroxyl group, was prepared and applied to an initiator of polymerization as the first step. The tetrahydropyranyl (THP) group is one of the useful protecting species of hydroxyl group, and shows both easy installation and general stability under nonacidic condition (*20*). Moreover, after the acid-catalyzed hydrolysis of THP, the deprotected hydroxyl group can then be devoted to further derivatization (Scheme 1).

* To whom correspondence should be addressed. Professor Kazunori Kataoka, Tel: +81-3-5841-7138. Fax: +81-3-5841-7139, e-mail: kataoka@bmw.t.u-tokyo.ac.jp.

[†] Graduate School of Engineering, The University of Tokyo, and CREST, JST.

[‡] Center for NanoBio Integration, The University of Tokyo.

[§] Graduate School of Medicine, The University of Tokyo.

10.1021/bc900253p
Published on Web 01/15/2010

Scheme 1. Synthetic Route to Heterobifunctional PEG Derivatives Possessing Azido and Alkyne Functional Groups

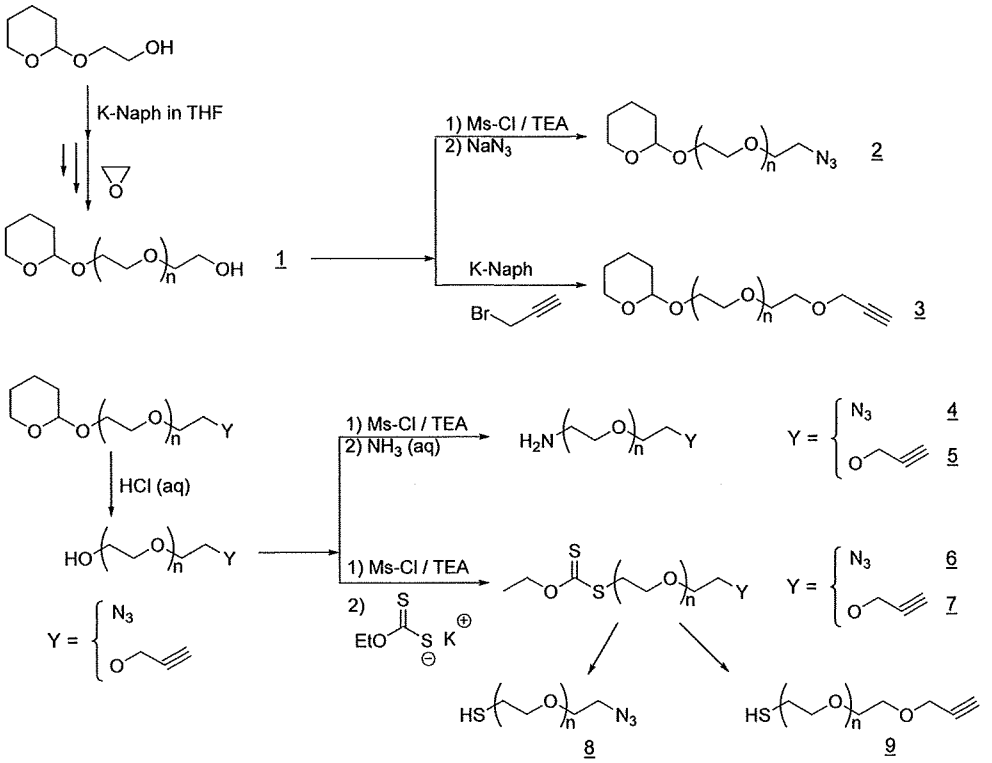

EXPERIMENTAL PROCEDURES

Materials. 2-(Tetrahydro-2*H*-pyran-2-yloxy)ethanol (Fluka, US) and ethylene oxide (EO; Sumitomo Seika Chemical, Japan) were dried over calcium hydride and distilled under an argon atmosphere. Potassium naphthalene was prepared as a tetrahydrofuran (THF) solution according to a previous paper (*21*), whose concentration was determined by titration. *N,N*-Dimethylformamide (DMF), THF, triethylamine (TEA), and methanesulfonyl chloride (Ms-Cl) were purchased from Wako Pure Chemical Industries, Ltd., (Osaka, Japan) and purified by conventional methods. Ammonia solution (ca. 25% (NH_3)), propargyl bromide in toluene solution (80 wt %), sodium azide, potassium ethyl xanthogenate, and other reagents were used as received.

Synthesis of THP-PEG-OH (1). General procedure: monoprotected ethylene glycol, 2-(tetrahydro-2*H*-pyran-2-yloxy)ethanol (1.43 mmol, 195 μL), and potassium naphthalene (1.23 mmol) in 4.1 mL of THF were added to dry THF (90 mL) in a 200 mL flask equipped with a three-way stopcock under argon atmosphere to form potassium alcoholate as an initiator. After stirring for 10−15 min, liquid EO (381 mmol, 16.8 g) was added to the solution via a cooled syringe. The mixture was allowed to react for 48 h at 25 °C and followed by a pouring into diethyl ether to precipitate the polymer. The recovered polymeric sample was dried in vacuo and then freeze−dried from benzene. The yield of obtained polymer was 97% (16.2 g). GPC: number-average molecular weight (M_n) = 11 500, M_w/M_n = 1.03. ^{1}H NMR (500 MHz, $CDCl_3$, δ in ppm): 1.46−1.83 (m, CH-(C*H*$_2$)$_3$-CH_2 of THP), 3.85 (t, CH-$(CH_2)_3$-C*H*$_2$-O of THP), 4.59 (t, O−C*H*-O of THP).

Synthesis of THP-PEG-Azide (2). The azide end group was introduced by the mesylation of the hydroxyl terminus and subsequent substitution with sodium azide, according to the previous method (*19*).

Freeze−dried polymer **1** (THP-PEG-OH) (1.13 g, 0.20 mmol) from benzene (30 mL) was dissolved in anhydrous THF (15 mL) followed by the addition of TEA (102 mg, 1.01 mmol). The mixture was then added to a solution of Ms-Cl (102 mg, 0.89 mmol) in THF (3 mL) under Ar stream, and stirred overnight at room temperature. After the reaction, the polymer was recovered by precipitation into ether and dried in vacuo, yielding a white solid.

This mesylated polymer (1.00 g, 0.15 mmol) was dissolved in DMF (12 mL), followed by sodium azide (400 mg, 6.15 mmol) addition, and was stirred at 45 °C for 3 days. After the reaction, DMF was partially evaporated and diluted with water (40 mL), then extracted by dichloromethane (6 × 120 mL). The combined organic layer was dried over $MgSO_4$, filtered, concentrated, and then reprecipitated into ether. The recovered polymer was freeze−dried from benzene. (0.83 g, 83%). ^{1}H NMR (500 MHz, $CDCl_3$, δ in ppm): 1.46−1.85 (m, CH-(C*H*$_2$)$_3$-CH_2 of THP), 3.46 (t, CH_2-C*H*$_2$-N_3), 3.85 (t, CH-$(CH_2)_3$-C*H*$_2$-O of THP), 4.59 (t, O-C*H*-O of THP).

Synthesis of THP-PEG-Alkyne (3). To prepare THP-PEG-Alkyne (**3**), modification of hydroxyl group of polymer **1** and the removal of unalkynated PEG was performed. Polymer **1** (THP-PEG-OH, 1.50 g, 0.25 mmol) was freeze−dried from benzene and dissolved in anhydrous THF (15 mL). Subsequently, potassium naphthalene solution was added until the solution turned pale green to reactivate the chain end and stirred for 15 min. To the solution was added propargyl bromide (299 mg, 2.51 mmol) as toluene solution, and the reaction mixture was stirred at room temperature for 48 h. Then, the polymer was recovered by precipitation into ether twice and dried by freeze−drying with benzene. 1.35 g (0.23 mmol) of the resulting polymer was dissolved in dichloromethane (3 mL), followed by the addition of pyridine (1 mL). After the stirring for 1.5 h, 2 mL of solution of succinic anhydride (40 mg, 0.40 mmol) in dichloromethane was introduced and reacted at 30 °C for 24 h. To quench the remaining succinic anhydride, ethanol (about 1 mL) was added and stirred for another 24 h. The resulting polymer was recovered by precipitation into ether and dried in

vacuo. To isolate THP-PEG-Alkyne (**3**), this polymer mixture was dissolved in the mixed-solvent (H_2O/acetonitrile = 4/1 v/v) and separated through an ion exchange column (DEAE-Sephadex). Further purification was carried out by dialyzing against distilled, deionized water using a Spectrapro dialysis membrane (MW cutoff 3500) and then freeze−drying to obtain THP-PEG-Alkyne (**3**) (535 mg, 40%). ^{1}H NMR (300 MHz, $CDCl_3$, δ in ppm): 1.46−1.85 (m, CH-(C$\underline{H}_2$)$_3$-CH_2 of THP), 2.43 (t, C$\underline{H}$ of Alkyne), 4.20 (s, O-C$\underline{H}_2$-C of Alkyne), 4.59 (t, O-C$\underline{H}$-O of THP).

Deprotection of THP Group. A 1.0 g sample of the THP-ended PEG (**2** or **3**) was dissolved into methanol (ca. 15 mL), and 4−5 drops of 1 mol/L hydrochloric acid (HCl) aqueous solution was added. After stirring around 4 h at ambient temperature, the reaction mixture was poured into ether to precipitate the PEG sample. The recovered polymer was washed with ether carefully and dried in vacuo. The removal of the THP group was confirmed by ^{1}H NMR spectroscopy.

Amination Reaction of HO-PEG-Y (Y = N_3 and OCH_2−C≡CH). To prepare amino-terminated heterobifunctional PEG, NH_2-PEG-Azide, or NH_2-PEG-Alkyne, two-step modification was performed: activation of hydroxyl group by methanesulfonyl ester formation and substitution with ammonia. In the first step, the mesylation reaction of the resultant polymer, HO-PEG-Y (Y = N_3 and OCH_2−C≡CH), was carried out according to the same procedure as described above. After precipitation into ether, filtration, and freeze−drying from benzene, the mesylated polymer was mixed with 25 wt % ammonia aqueous solution and stirred at room temperature for about 4 days. After the reaction, to remove excess ammonia, the mixture was partially evaporated and dialyzed first against diluted ammonia solution (ca. 0.125 N in H_2O) and then against distilled water using a Spectrapro dialysis membrane (MW cutoff 3500). Lyophilization of the dialyzed solution gave the amine-functionalized polymer, NH_2-PEG-Y (Y = N_3 (**4**) and OCH_2−C≡CH (**5**)).

Synthesis of Dithiocarbonate Introduced HO-PEG-Y (Y = N_3 (6) and OCH_2−C≡CH (7)). To derivatize HO-PEG-Y (Y = N_3 and OCH_2−C≡CH) with dithiocarbonate moiety, preparation of the methanesulfonyl ester of the polymer and subsequent substitution with potassium ethyl xanthogenate was carried out according to a previous report (*22*). The mesylation reaction of the resultant polymer, HO-PEG-Y (Y = N_3 and OCH_2−C≡CH), was carried out according to the same procedure as described above. After the precipitation into ether, filtration, and freeze−drying from benzene, the mesylated HO-PEG-OCH_2-C≡CH (207 mg) was dissolved in THF (20 mL). After the stirring for 20 min, 4 mL of cosolvent (THF/DMF = 5/5 vol %) containing potassium xanthogenate (111 mg, 0.69 mmol) was added and stirred at room temperature for 10 h. The reaction mixture was then mixed with dichloromethane (100 mL) and washed with a saturated NaCl aqueous solution several times. The organic layer was dried over $MgSO_4$, filtered, concentrated, and then reprecipitated into ether. The recovered polymer, CH_3CH_2-O-(C=S)-S-PEG-OCH_2-C≡CH was freeze−dried from benzene (176 mg, 85%). To introduce the *O*-ethyldithiocarbonate group at the hydroxyl terminus of HO-PEG-N_3, the same procedure was performed. After freeze−drying, the yield of the recovered sample was determined to be 83%.

Synthesis of HS-PEG-Y (Y = N_3 (8) and OCH_2-C≡CH (9)). To prepare the thiol-terminated PEG derivatives, HS-PEG-Y (Y = N_3 and OCH_2−C≡CH), simple reaction with propylamine (*22*) or sodium hydroxide solution was conducted. The azido-terminated PEG containing dithiocarbonate moiety (polymer **6**) (100 mg) was dissolved in methanol (2 mL), and sodium hydroxide (66 mg) aqueous solution (500 μL) was slowly added. The mixture was stirred for 12 h at room temperature and then dialyzed against distilled water. After the lyophilization of the dialyzed solution, the thiolated sample, HS-PEG-N_3 (**8**) was obtained as white powder (86 mg, yield = 86%). ^{1}H NMR (500 MHz, $CDCl_3$, δ in ppm): 2.88 (t, CH_2-C$\underline{H}_2$-SH and C$\underline{H}_2$-SS-C$\underline{H}_2$), 3.49 (t, CH_2-C$\underline{H}_2$-N_3).

Thiolation reaction of alkyne-terminated sample (polymer **7**) was performed by reference to the previous method (*22*). Polymer **7** (40 mg) was dissolved in THF (1 mL) and reacted with propylamine (100 μL) at room temperature. After the reaction for 3 h, the polymer solution was dialyzed against MeOH followed by the complete evaporation of the solvent under vacuum. The polymer was purified by reprecipitation into cold ether and dried in vacuo (33 mg, yield = 80%). ^{1}H NMR (500 MHz, $CDCl_3$, δ in ppm): 2.44 (t, C$\underline{H}$ of Alkyne), 2.88 (t, CH_2-C$\underline{H}_2$-SH and C$\underline{H}_2$-SS-C$\underline{H}_2$), 4.20 (s, O-C$\underline{H}_2$-C of Alkyne).

Table 1. Results of Ring-Opening Polymerization of EO[a]

run	[M]/[I]	yield[b] (%)	$10^{-3} \times M_n$ calcd	$10^{-3} \times M_n$ GPC[c]	$10^{-3} \times M_n$ MS[d]	M_w/M_n[c]
1	100	96	4.4	4.2	4.5	1.04
2	136	97	6.0	5.9	6.1	1.03
3	264	97	11.7	11.5	11.7	1.03

[a] Polymerization was conducted in THF at 25 °C for 48 h. [b] After reprecipitation into ether. [c] Determined by GPC (DMF eluent) calibrated with commercial PEO standards. [d] Determined by MALDI-TOF MS spectra.

Polymer Analysis. ^{1}H NMR spectra were recorded on JEOL JNM-AL (300 MHz) or JEOL Alpha series (500 MHz) spectrometer (JEOL, Tokyo, Japan). ^{13}C NMR spectra were recorded on JNM-AL model at 75.45 MHz. Chemical shifts are reported in parts per million (ppm) downfield from tetramethylsilane. Number-average molecular weight (M_n) and molecular weight distribution (M_w/M_n) were determined using a GPC (TOSOH HLC-8220) system equipped with two TSK gel columns (G4000HHR and G3000HHR) and an internal refractive index (RI) detector. Columns were eluted with DMF containing lithium chloride (10 mM) with a flow rate of 0.8 mL/min and at a temperature of 40 °C. Molecular weights were calibrated with poly(ethylene glycol) standards (Polymer Laboratories, Ltd., UK). MALDI-TOF-MS spectra were recorded using Bruker REFLEX III. α-Cyano-4-hydroxycinnamic acid was used as the matrix for the ionization operated in the reflection mode.

RESULTS AND DISCUSSION

Although the hydroxyl group does not show high reactivity in itself comparing with other functional groups, the hydroxyl group can be converted to useful reactive groups through the activation and subsequent nucleophilic substitution. Hence, the availability of the hydroxyl group is potentially high. If homotelechelic HO-PEG-OH is used as a starting material for the preparation of heterobifunctional PEG derivatives, however, undesired yield of homobifunctional product and multiple column purification process are inevitable. Here, we designed a simple synthetic procedure containing preparation of hydroxyl-terminated PEG as the intermediate, of which one hydroxyl group is protected quantitatively, and alternating functionalization of both terminal ends.

Preparation of Monoprotected PEG via Polymerization of EO. In this study, monotetrahydropyranylated ethylene glycol derivative, 2-(tetrahydro-2*H*-pyran-2-yloxy)ethanol, was selected as an initiator for anionic polymerization of EO, because the tetrahydropyranyl (THP) group is one of the useful protecting species of hydroxyl group (*20*), and shows both easy installation and general stability under nonacidic conditions. In other words, it is expected that the THP protecting group is stable under

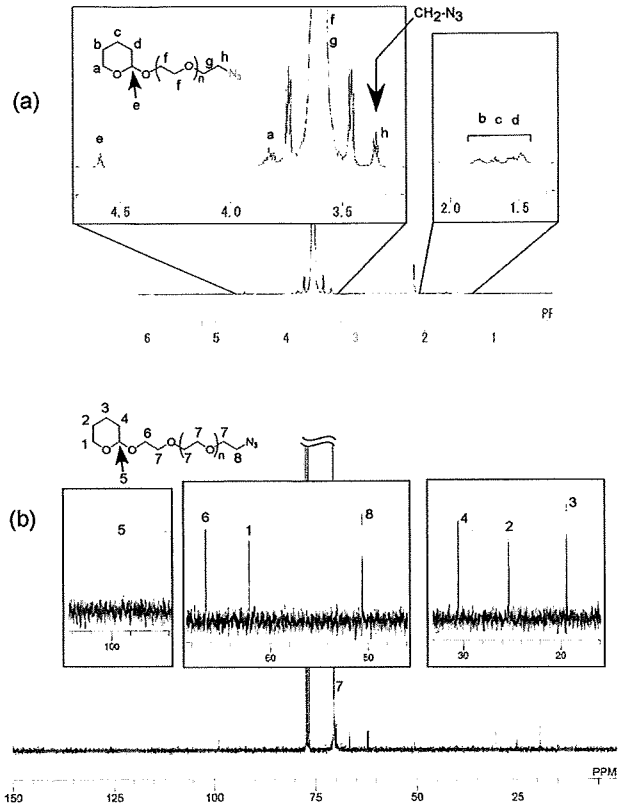

Figure 1. (a) 500 MHz ^{1}H NMR spectrum of THP-PEG-Azide (in $CDCl_3$ at 20 °C). (b) ^{13}C NMR spectrum of THP-PEG-Azide (in $CDCl_3$).

polymerization condition of EO and subsequent functionalization step with azide/alkyne. Table 1 shows the results of the polymerization of EO in the presence of monotetrahydropyranylated ethylene glycol as an initiator. All polymerization proceeded with excellent isolated yields of the polymeric samples (>96%), and the M_n values determined by GPC and MALDI-TOF MS showed good agreement with calculated values, indicating the controlled molecular weight of THP-PEG-OH (**1**) without any side reaction.

Azidation Reaction of THP-PEG-OH. To demonstrate the versatility of THP-PEG-OH (**1**), selective and quantitative modification of the ω-hydroxyl end was examined. First, the azidation reaction was conducted through the two-step modification, the mesylation and the substitution by sodium azide, of hydroxyl function as described in the Experimental Section.

In the ^{1}H NMR spectrum of the product after azidation (run 2 in Table 1), the proton signals of THP group are detected at δ 4.63 ppm (e), 3.86 ppm (a), and 1.46−1.85 ppm (b, c, d), respectively. In addition to these signals, the methylene unit adjacent to the azido group ($CH_2\underline{CH_2}N_3$ (h)) was observed at 3.39 ppm (Figure 1a). With comparison of the integral ratio of proton signals at α- (δ 4.63 ppm (e)) and ω-ends (δ 3.39 ppm (h)), the quantitative conversion from the hydroxyl to the azido group was indicated. Additionally, the ^{13}C NMR spectrum shows that the methylene and methyne signals of the THP structure are detected around δ 99.4 ppm (C5), 65.3, ppm (C6), 62.0 ppm (C1), 30.3 ppm (C4), 25.4 ppm (C2), and 19.7 ppm (C3), respectively (Figure 1b). Moreover, no signal of the methylene carbon adjacent to the hydroxyl terminus ($CH_2\underline{C}H_2OH$: δ = 61.5 ppm) (*23*) was detected. These results strongly support the quantitative introduction of azido functionality at the ω-end of THP-PEG-OH.

Preparation of THP-PEG-Alkyne (3). To represent the selective derivatization of THP-PEG-OH (**1**) applicable to "click chemistry", the introduction of alkyne moiety, the counterpart of azide/alkyne cycloaddition reaction, was studied. For alkynation of the hydroxyl group of THP-PEG-OH, Williamson's ether synthetic method with propargyl bromide was performed after the formation of alcolate by the addition of potassium naphthalene. From ^{1}H NMR analysis of the resulting product, the proton signals of the

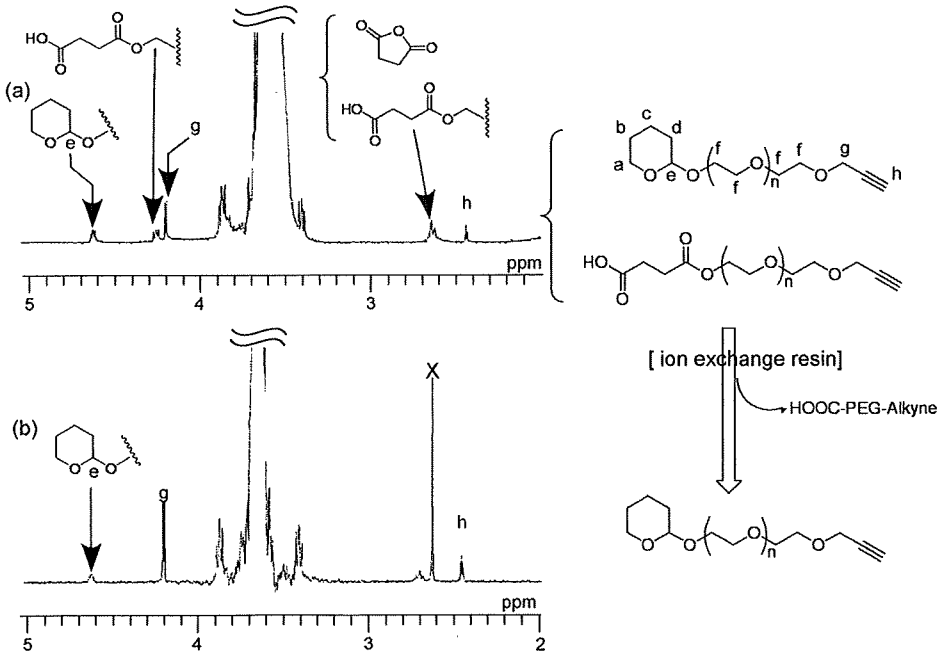

Figure 2. ^{1}H NMR spectra of alkyne-terminated PEGs; sample after the carboxylation reaction (a) and sample through DEAE-Sephadex resin column (b) (300 MHz in $CDCl_3$).

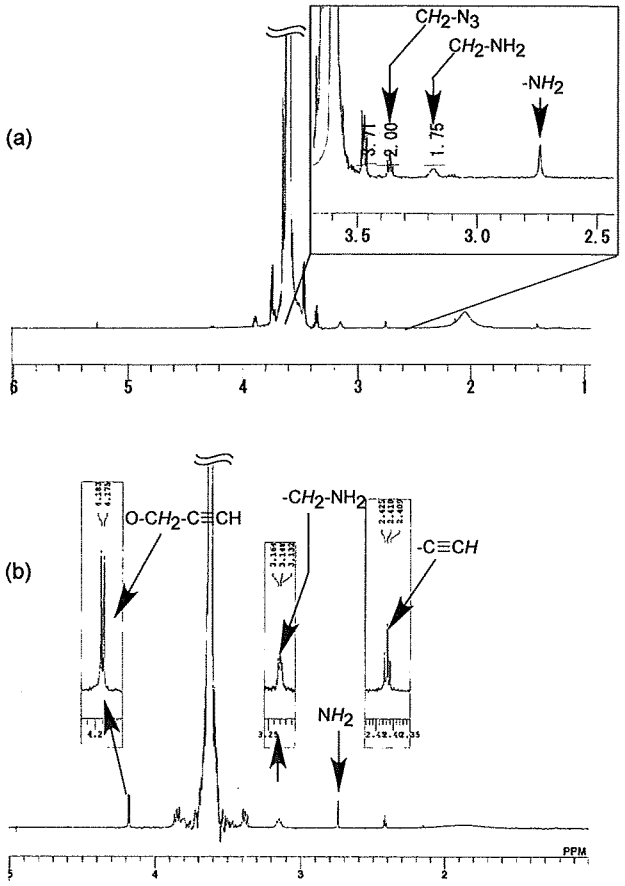

Figure 3. (a) 500 MHz ^{1}H NMR spectrum of NH_2-PEG-Azide (in $CDCl_3$). (b) ^{1}H NMR spectrum of NH_2-PEG-Alkyne (in $CDCl_3$).

alkyne moiety are detected at δ 2.43 ppm (h) and 4.20 ppm (g), respectively, with the signals assigned to the THP group, indicating the efficient alkynation (Figure 2a). However, the conversion rate of alkynation estimated by ^{1}H NMR analysis was relatively low (around 70%). The polymer sample with remaining THP-PEG-OH will yield the undesired byproduct, homobifunctional HO-PEG-OH, after the deprotection of the THP group. Then, separation of the unalkynated THP-PEG-OH from the sample was examined with simple column purification. After the carboxylation of the remaining hydroxyl group with succinic anhydride in dichloromethane, the polymer mixture was passed through the ion exchange column. The carboxylated PEG was separated from the mixture by ionic absorption with DEAE-Sephadex resin in a column, whereas the alkynated sample, THP-PEG-Alkyne, was eluted without retention. In the ^{1}H NMR spectrum of the sample after the dialysis and lyophilization, no signal based on the carboxylated PEG was observed, suggesting the effective removal of unalkynated fraction and isolation of the quantitative alkyne-functionalized THP-PEG.

Preparation of NH_2-PEG-Y (Y = N_3 (4) and OCH_2−C≡CH (5)). Removal of protective group, THP, will allow further derivatization of the α-terminal end of azido- or alkyne-terminated PEG. Deprotection of THP was carried out under acidic condition with diluted HCl, and ^{1}H NMR spectrum of the resulting sample indicated absence of the proton signals corresponding to the THP group (data not shown). To convert a hydroxyl group of the deprotected samples, HO-PEG-Azide and HO-PEG-Alkyne, to primary amino group, mesylation and subsequent nucleophilic substitution by ammonia was performed. In the ^{1}H NMR spectrum of aminated sample (Figure 3a), the characteristic methylene signals adjacent to both the azido group (-$C\underline{H}_2N_3$: δ = 3.36 ppm) and the primary amino group (-$C\underline{H}_2NH_2$: δ = 3.18 ppm) were clearly observed. Additionally, the amination degree estimated from the integral ratio of these proton signals was 85% and above, indicating successful preparation of NH_2-PEG-N_3. Likewise, the ^{1}H NMR spectrum of aminated HO-PEG-Alkyne exhibits the distinguishing signals assigned to both the alkyne moiety (C$\underline{H}$ of Alkyne: δ = 2.41 ppm and O-C$\underline{H}_2$-C of Alkyne: 4.18 ppm) and the primary amino group (-$C\underline{H}_2NH_2$: δ = 3.14 ppm) in Figure 3b. Moreover, to confirm the quantitative terminal functionalization of this alkyne-terminated PEG sample, the analysis by MALDI-TOF MS spectroscopy was also conducted. Figure 4 shows the MS spectrum of NH_2-PEG-Alkyne (5). The major series of the molecular masses of the product is expressed in the following equation

$$MW_{MS} = 44.053n(EO) + 39.05(\text{Alkyne moiety; } CH_2C \equiv CH) + 16.02(NH_2) + 22.99(\text{sodium})$$

In this analysis, only parent ions of each polymer molecule as expected are observed, without the signal assigned to the byproduct NH_2-PEG-NH_2. These data strongly support the successful preparation of NH_2-PEG-Alkyne (5).

Preparation of HS-PEG-Y (Y = N_3 (8) and OCH_2−C≡CH (9)). To demonstrate the versatility of this synthetic route based on THP-PEG-Y (Y = Azide and

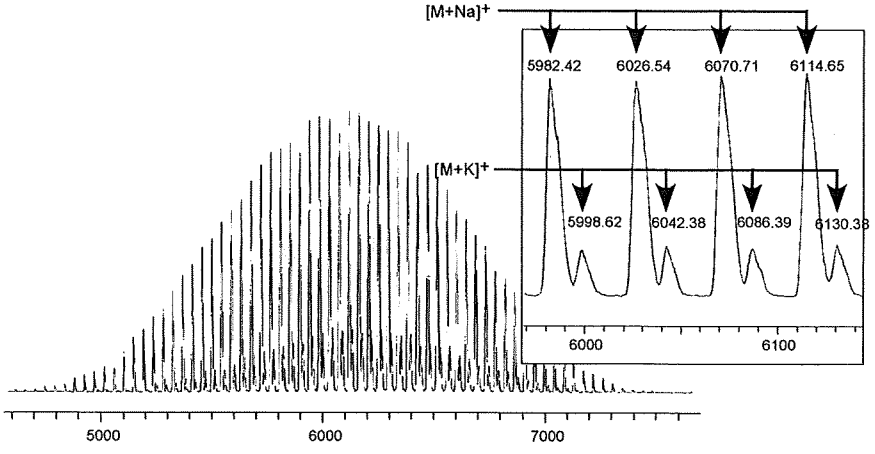

Figure 4. MALDI-TOF MS spectrum of NH_2-PEG-Alkyne.